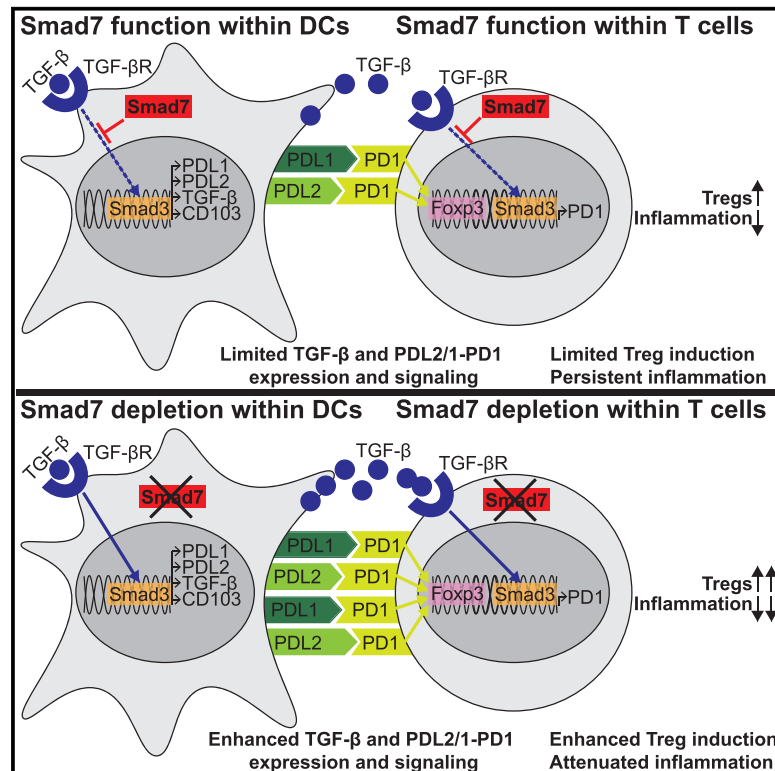


Smad7 Controls Immunoregulatory PDL2/1-PD1 Signaling in Intestinal Inflammation and Autoimmunity

Graphical Abstract



Authors

Lucien P. Garo, Amrendra K. Ajay, Mai Fujiwara, ..., Stephen Rubino, Howard L. Weiner, Gopal Murugaiyan

Correspondence

mgopal@rics.bwh.harvard.edu

In Brief

Smad7, a negative regulator of TGF- β signaling, is implicated in the pathogenesis and treatment of inflammatory bowel diseases (IBDs). Here, Garo et al. describe how Smad7 within both dendritic cells and CD4⁺ T cells limits PD1-mediated Treg induction to promote intestinal inflammation, providing additional therapeutic strategies for IBD intervention.

Highlights

- Within DCs, Smad7 inhibits PD1 ligands, CD103, and TGF- β , limiting Treg induction
- Within CD4⁺ T cells, Smad7 inhibits PD1, limiting PD1-mediated Treg differentiation
- Smad7 deficiency in DCs or T cells mitigates DSS and T cell transfer colitis models
- Smad7-antisense inhibitor, or agonizing PD1 via PDL1/2-Fc, ameliorates colitis



Smad7 Controls Immunoregulatory PDL2/1-PD1 Signaling in Intestinal Inflammation and Autoimmunity

Lucien P. Garo,¹ Amrendra K. Ajay,² Mai Fujiwara,¹ Vanessa Beynon,¹ Chantal Kuhn,¹ Galina Gabriely,¹ Supriya Sadhukan,¹ Radhika Raheja,¹ Stephen Rubino,¹ Howard L. Weiner,¹ and Gopal Murugaiyan^{1,3,*}

¹Ann Romney Center for Neurologic Diseases, Department of Neurology, Brigham and Women's Hospital and Harvard Medical School, Boston, MA 02115, USA

²Renal Division, Department of Medicine, Brigham and Women's Hospital and Harvard Medical School, Boston, MA 02115, USA

³Lead Contact

*Correspondence: mgopal@rics.bwh.harvard.edu

<https://doi.org/10.1016/j.celrep.2019.07.065>

SUMMARY

Smad7, a negative regulator of TGF- β signaling, has been implicated in the pathogenesis and treatment of inflammatory bowel diseases (IBDs), including Crohn's disease (CD) and ulcerative colitis (UC). Here, we found that Smad7 mediates intestinal inflammation by limiting the PDL2/1-PD1 axis in dendritic cells (DCs) and CD4⁺T cells. Smad7 deficiency in DCs promotes TGF- β responsiveness and the co-inhibitory molecules PDL2/1 on DCs, and it further imprints T cell-PD1 signaling to promote Treg differentiation. DC-specific Smad7 deletion mitigates DSS-induced colitis by inducing CD103⁺PDL2/1⁺DCs and Tregs. In addition, Smad7 deficiency in CD4⁺T cells promotes PD1 and PD1-induced Tregs *in vitro*. The transfer of Smad7-deficient CD4⁺T cells enhances Tregs *in vivo* and protects against T cell-mediated colitis. Furthermore, Smad7 antisense ameliorates DSS-induced UC, increasing TGF- β and PDL2/1-PD1 signaling. Enhancing PD1 signaling directly via Fc-fused PDL2/1 is also beneficial. Our results identify how Smad7 mediates intestinal inflammation and leverages these pathways therapeutically, providing additional strategies for IBD intervention.

INTRODUCTION

Although the etiology of inflammatory bowel diseases (IBDs) such as Crohn's disease (CD) and ulcerative colitis (UC), remains unclear, exaggerated immune responses to the gut microbiota are thought to perpetuate the disease (Dalal and Chang, 2014). Among the regulatory mechanisms that prevent pathogenic inflammation, Foxp3-expressing regulatory CD4⁺T (Treg) cells are critical for controlling aberrant immune responses in the gut (Boden and Snapper, 2008; Izcue et al., 2009; Tanoue et al., 2016). The gut environment appears to be a preferential site for Treg development, reflecting the high immune challenge

and continuous need for immune suppression (Harrison and Powrie, 2013). Dendritic cells (DCs) play a central role in regulating these intestinal responses (Manicassamy and Pulendran, 2011; Rescigno and Di Sabatino, 2009). In particular, CD103⁺ DCs exhibit an enhanced ability to induce Tregs (Jaensson et al., 2008; Ruane and Lavelle, 2011). Dysfunction and reduced frequencies of intestinal CD103⁺ DCs and Tregs have been observed in IBD patients and animal models (Eastaff-Leung et al., 2010; Kourepini et al., 2014; Matsuno et al., 2017; Wenzel et al., 2014). Although DC-T cell dysfunction is a major factor underlying exaggerated immune responses in IBD, the mechanisms that limit regulatory DCs and Tregs in the gut are incompletely understood.

Programmed death 1 (PD1) and its ligands, PDL1 and PDL2, have emerged as critical inhibitory pathways that regulate T cell responses and maintain immune tolerance (Fife and Bluestone, 2008; Francisco et al., 2010; Sharpe et al., 2007). PD1 is expressed on CD4⁺T cells, while PDL1 and PDL2 are expressed on antigen-presenting cells (APCs), such as DCs. One major mechanism by which PD1 induces tolerance is by promoting Foxp3⁺Tregs when engaged to PDL1-expressing APCs (Francisco et al., 2009; Liu et al., 2013). Defective PDL1 expression in intestinal APCs has been observed in IBD patients, and blocking PD1 can promote intestinal inflammation in mice and humans (Bertha et al., 2017; Reynoso et al., 2009; Robertson et al., 2016; Scandiuzzi et al., 2014; Wang et al., 2017). Although PDL1-PD1 signaling has been shown to be critical for the control of intestinal inflammation, the contribution of PDL2 in intestinal Treg differentiation and the molecular pathways that control PDL2/1-PD1-mediated Treg differentiation in IBDs remain unclear.

Smad7, an inhibitor of regulatory transforming growth factor β (TGF- β) signaling, has been heavily implicated in IBDs. Elevated colonic Smad7 has been associated with enhanced inflammation in IBD patients (Monteleone et al., 2001, 2005). Knock down of Smad7 with a specific antisense oligonucleotide has been shown to resolve multiple sources of inflammation in mice and has yielded mixed results in IBD patients (Boirivant et al., 2006; Feagan et al., 2018; Kleiter et al., 2007; Lowe, 2017; Marafini et al., 2017; Monteleone et al., 2015). However, Smad7 inhibition and therapeutic studies have been hindered



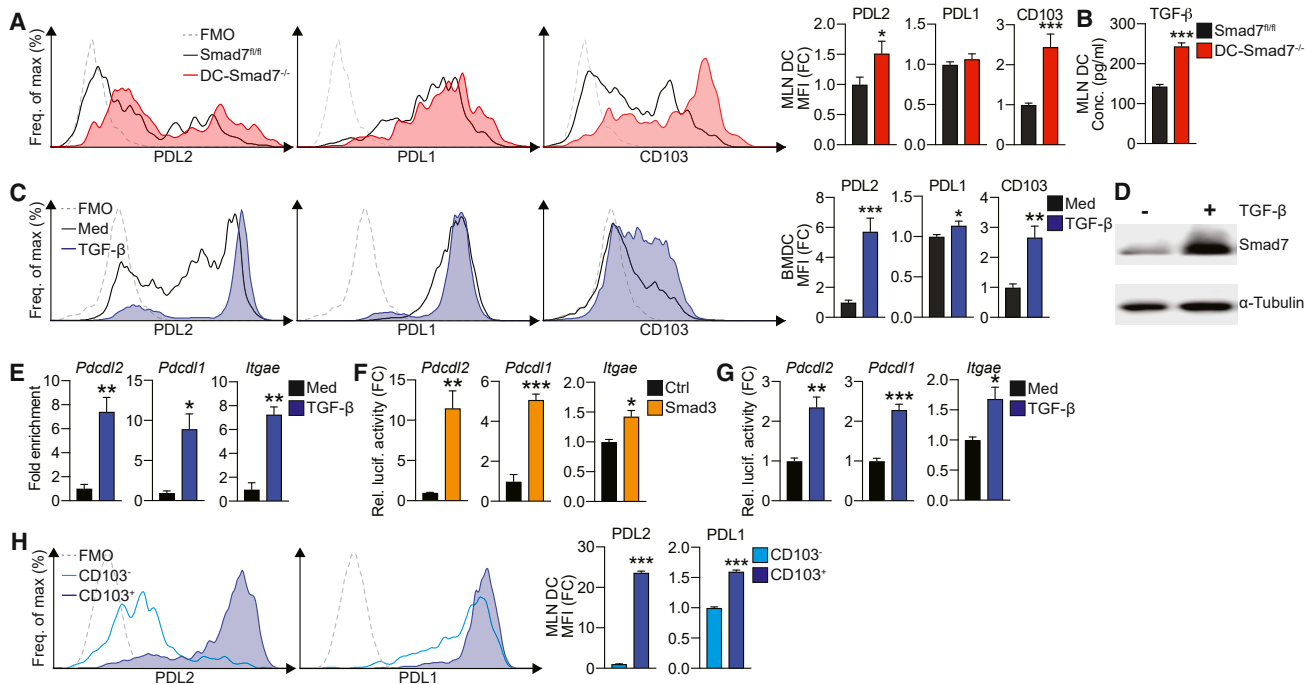


Figure 1. Smad7 Deficiency Promotes a PDL2⁺CD103⁺ Regulatory Phenotype in DCs

(A) Representative fluorescence-activated cell sorting (FACS) histograms (left) and median fluorescence intensities (MFIs) (right) of PDL2, PDL1, and CD103 in CD11c⁺ MLN DCs from naive Smad7^{fl/fl} and DC-Smad7^{-/-} mice (n = 11). (B) ELISA quantification of secreted TGF- β by MLN DCs from these mice (n = 4). (C) Representative FACS histograms (left) and MFIs (right) of PDL2, PDL1, and CD103 in CD11c⁺ BMDCs generated with or without TGF- β (30 ng/mL) from WT mice (n = 5). (D) Western blot of Smad7 in WT CD11c⁺ BMDCs stimulated with or without TGF- β (2.5 ng/mL) for 30 min. (E) ChIP analysis of Smad3 binding promoter regions of *Pdcd2* (PDL2), *Pdcd1* (PDL1), and *Itgae* (CD103) in WT CD11c⁺ DCs stimulated with or without TGF- β (10 ng/mL). ChIP data expressed as fold enrichment as compared to input control (n = 3). (F and G) Luciferase reporter activity of *Pdcd2*, *Pdcd1*, and *Itgae* promoters in HEK293 cells stimulated (F) with control or Smad3 construct or (G) with or without TGF- β (2 ng/mL) (n = 3). Luciferase activity as relative activity fold change (FC) from (F) control or (G) media condition. (H) Representative FACS histograms (left) and MFIs (right) of PDL2 and PDL1 in CD103⁺ and CD103⁻ MLN CD11c⁺ DCs from WT mice (n = 4). Data representative of ≥ 3 independent experiments. MFI data reflective of CD11c⁺ population and expressed as FC from (A) Smad7^{fl/fl} condition, (C) media condition, or (H) CD103⁻ condition. Means \pm SEMs. *p < 0.05, **p < 0.01, and ***p < 0.001 by unpaired t test. See also Figure S1.

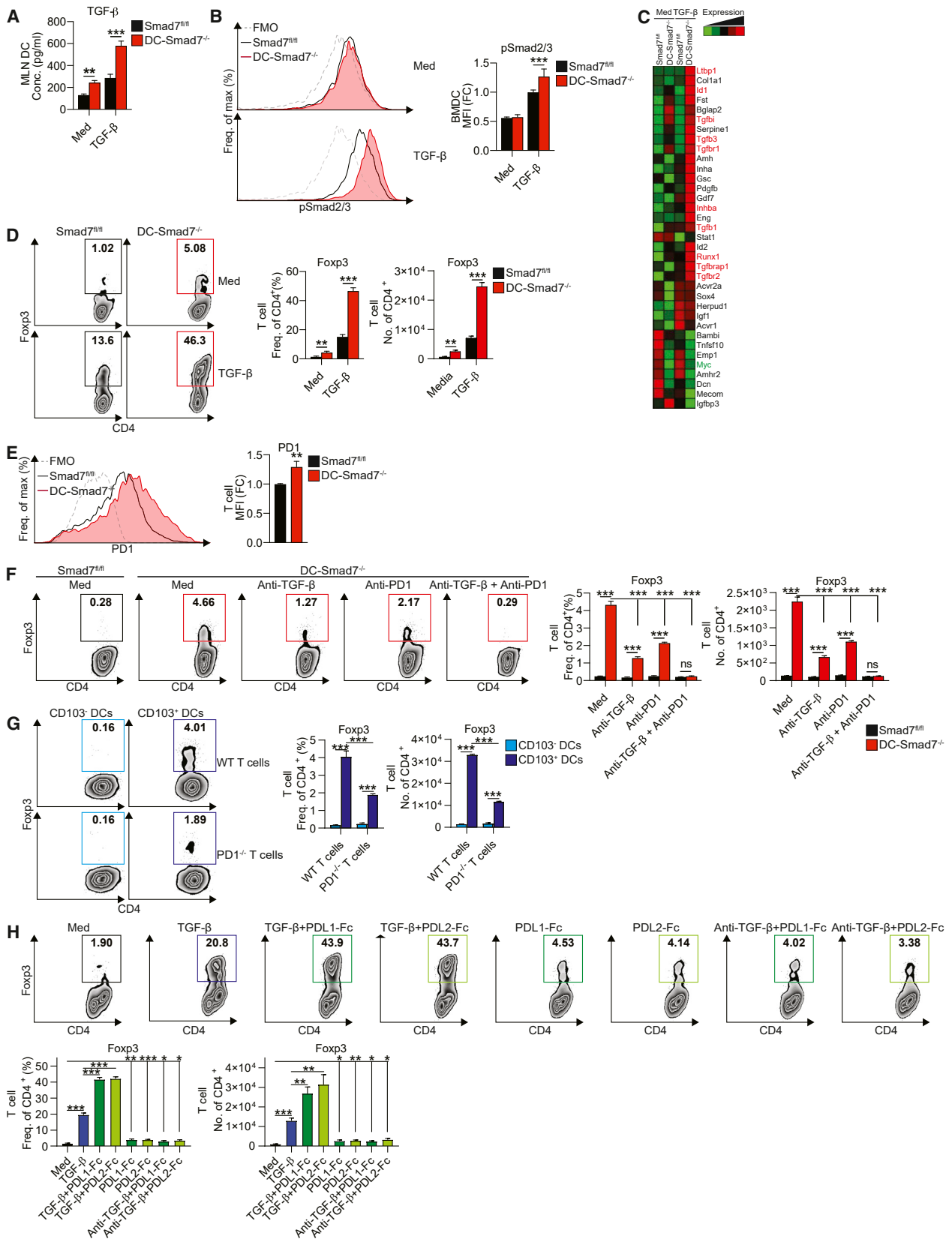
by the fact that the molecular pathways by which Smad7 mediates its pathogenic functions in IBDs, including its cell type-specific functions, remain poorly understood.

Here, we uncovered a role for Smad7 in mediating intestinal inflammation by limiting PDL2/1-PD1 signaling. Our results suggest that Smad7 sustains detrimental immune responses in IBDs by inhibiting the PDL2/1-PD1 axis within both DCs and CD4⁺ T cells. Specific deletion of Smad7 within DCs and T cells protects mice from intestinal inflammation and is associated with increased TGF- β responsiveness, PDL2/1-PD1 signaling, and Treg differentiation. We also demonstrate that silencing Smad7 ameliorates dextran sodium sulfate (DSS)-induced colitis and is associated with increased TGF- β and PDL2/1-PD1 signaling. Finally, we show that enhancing PD1 signaling directly via the administration of recombinant Fc-fused PDL1 or PDL2 is effective in mitigating colitis. Our results identify previously unknown mechanisms by which Smad7 mediates intestinal inflammation and establishes how these insights could be leveraged therapeutically in patients with IBDs.

RESULTS

Smad7 Deficiency Promotes the Development of CD103⁺ PDL2⁺ Regulatory DCs

To study the effect of Smad7 on DCs, we generated mice deficient in Smad7 in CD11c⁺ DCs (DC-Smad7^{-/-}) (Figure S1A). We saw a minor increase in CD11c⁺ DC frequency (Figure S1B) and no change in DC co-stimulatory molecule expression (Figure S1C). Notably, we found that mesenteric lymph node (MLN) DCs from DC-Smad7^{-/-} mice present with a regulatory phenotype, expressing much higher levels of PD1 ligand, PDL2, and CD103 (Figure 1A). This was observed in both CD11c⁺CD11b⁻ and CD11c⁺CD11b⁺ populations in the gut (data not shown; Muzaki et al., 2016). Similarly, bone marrow-derived DCs (BMDCs) from DC-Smad7^{-/-} mice generated *in vitro* show enhanced PDL2 and CD103, with no significant difference in other co-stimulatory molecules (Figure S1D). Since we found that Smad7^{-/-} DCs secrete more TGF- β (Figure 1B), we asked whether TGF- β could be inducing the regulatory



(legend on next page)

phenotype we observed. For this, we generated BMDCs in the presence or absence of TGF- β and found that BMDCs generated with TGF- β also express increased PDL2 and CD103 and moderately higher PDL1 (Figure 1C). In contrast, blocking TGF- β inhibits PDL2 and CD103, while moderately reducing PDL1 in DCs (Figure S1E). Similar to the effects observed in other cell types (Afrakhte et al., 1998; Tang et al., 2009), we found that the stimulation of DCs by TGF- β results in increased Smad7, a negative regulator of TGF- β signaling that inhibits Smad2 and Smad3 (Figure 1D).

Since DCs generated in the presence of TGF- β *in vitro* and DCs lacking a negative regulator of TGF- β generated *in vivo* show enhanced expression of PDL2 and CD103 and a moderate increase in PDL1, we asked whether TGF- β -induced Smad transcription factors are involved in the transcriptional activation of PDL2, PDL1, and CD103 genes. We performed a transcription factor binding site (TFBS) analysis for the promoter regions of human and mouse *Pdcd2* (PDL2), *Pdcd1* (PDL1), and *Itgae* (CD103) genes and found multiple putative Smad3 binding sites on all three (Figure S1F). To confirm that Smad3 binds these promoters, we performed chromatin immunoprecipitation (ChIP) assays with Smad3 antibody using DCs stimulated with or without TGF- β . We found significantly increased binding of Smad3 to all three gene promoters from TGF- β -stimulated DCs (Figure 1E). To further investigate TGF- β on the Smad3-dependent transcriptional regulation of these genes, we performed reporter assays using constructs in which a PDL2, PDL1, or CD103 promoter sequence was cloned upstream of a luciferase gene. Transfection of Smad3 cDNA construct in HEK293 cells transactivates PDL2, PDL1, and CD103 promoters, as shown by increased luciferase expression (Figure 1F). In addition, the upregulation of endogenous Smad3 by TGF- β stimulation also induces promoter binding (Figure 1G). Consistent with a role for Smad3 in the transcriptional activation of PDL2, PDL1, and CD103, we found BMDCs and *ex vivo*-isolated splenic and MLN DCs from Smad3-deficient (*Smad3*^{-/-}) mice express significantly lower levels of PDL2, PDL1, and CD103 (Figures S1G and S1H). In contrast to *Smad7*^{-/-} DCs (Figure 1B), these DCs also express less TGF- β (Figure S1I).

Based on observations that CD103⁺ DCs express increased levels of TGF- β and that TGF- β transcriptionally regulates PDL2, PDL1, and CD103, we asked whether these tolerogenic markers are regulated concomitantly *in vivo* under normal conditions. For this, we evaluated the expression of PDL2/1 in CD103⁺ and CD103⁻ MLN DC populations in wild-type (WT) mice. We found that PDL2 is highly associated with CD103, while PDL1 correlates less robustly (Figure 1H). This pattern is analogous to the stark and modest upregulation of PDL2 and PDL1, respectively, in response to TGF- β (Figure 1C). Together, these findings suggest that TGF- β stimulation induces a tolerogenic transcriptional program in DCs, which is enhanced by the absence of Smad7.

Smad7 Restricts the Responsiveness of DCs to TGF- β Stimulation

TGF- β has been shown to induce its own expression in multiple cell types, including DCs (Bouché et al., 2000; Kashiwagi et al., 2015). Smad7 negatively regulates TGF- β signaling by inhibiting Smad2 and Smad3 phosphorylation, two major transcription factors downstream of TGF- β signaling (Shi and Massagué, 2003). Based on our observations of enhanced expression of regulatory markers and TGF- β in *Smad7*^{-/-} DCs, both of which are induced by TGF- β stimulation, we tested whether Smad7 restricts the responsiveness of DCs to TGF- β . We found that autocrine induction of TGF- β is amplified in the absence of Smad7 in DCs (Figure 2A). Consistent with this, increased phosphorylation of Smad2 and Smad3 is measured in *Smad7*^{-/-} DCs in response to TGF- β (Figure 2B). Correspondingly, autocrine induction of TGF- β is completely impaired in *Smad3*^{-/-} DCs (Figure S2A). In addition, our TGF- β signaling array identified the upregulation of assorted TGF- β -responsive genes in *Smad7*^{-/-} DCs (Figure 2C). These results show that Smad7 deficiency in DCs promotes responsiveness to TGF- β stimulation.

Smad7^{-/-} DCs Promote the Differentiation of Naive CD4⁺ T Cells Into Foxp3⁺ Tregs

Given the enhanced TGF- β levels and regulatory surface markers of *Smad7*^{-/-} DCs, we then investigated whether this

Figure 2. Smad7 Restricts DC Responsiveness to TGF- β and Their Ability to Induce Tregs

(A) ELISA quantification of secreted TGF- β from *Smad7*^{fl/fl} and *Smad7*^{-/-} MLN CD11c⁺ DCs stimulated with or without TGF- β (0.5 ng/mL), for 12 h, washed, and cultured for another 48 h (n = 4).

(B) Representative FACS histograms (left) and MFIs (right) of phospho-Smad2/3 in BMDCs stimulated with or without TGF- β (2 ng/mL), for 1 h (n = 6).

(C) qRT-PCR (using Qiagen Mouse TGF- β Signaling Pathway RT2 Profiler PCR Array) of TGF- β and associated TGF- β signaling molecules in *Smad7*^{fl/fl} and *Smad7*^{-/-} CD11c⁺ DCs stimulated with or without TGF- β (10 ng/mL), for 10 h.

(D) Representative FACS plots (left), frequencies (center), and cell counts per well (right) of Foxp3-GFP⁺ populations in naive CD4⁺ Foxp3-GFP T cells co-cultured with MLN CD11c⁺ DCs from *Smad7*^{fl/fl} or DC-*Smad7*^{-/-} mice at a 1:3 DC:T cell ratio, with or without TGF- β (0.5 ng/mL), for 4 days (n = 8).

(E) Representative FACS histograms (left) and frequencies (right) of PD1 in naive CD4⁺ T cells co-cultured with MLN CD11c⁺ DCs from *Smad7*^{fl/fl} or DC-*Smad7*^{-/-} mice at a 1:3 DC:T cell ratio, for 18 h.

(F) Representative FACS plots (left), frequencies (center), and cell counts per well (right) of Foxp3-GFP⁺ populations in naive CD4⁺Foxp3-GFP T cells co-cultured with MLN CD11c⁺ DCs from *Smad7*^{fl/fl} or DC-*Smad7*^{-/-} mice at a 1:3 DC:T cell ratio, with or without anti-TGF- β (10 μ g/mL) and/or anti-PD1 (10 μ g/mL), for 4 days (n = 3).

(G) Representative FACS plots (left), frequencies (center), and cell counts per well (right) of Foxp3⁺ populations in naive CD4⁺ T cells from WT or PD1-deficient mice co-cultured with CD103⁻ or CD103⁺ DCs from WT mice at a 1:3 DC:T cell ratio, for 3 days (n = 3).

(H) Representative FACS plots (top), frequencies (bottom left), and cell counts per well (bottom right) of Foxp3-GFP⁺ populations in naive CD4⁺Foxp3-GFP T cells stimulated with or without TGF- β (0.5 ng/mL), recombinant plate-bound PDL1-Fc or PDL2-Fc (30 μ g/mL), and/or anti-TGF- β (10 μ g/mL), for 4 days (n = 6).

MFI data reflective of (B) CD11c⁺ or (E) CD4⁺ populations and expressed as FC from *Smad7*^{fl/fl} condition. Data representative of ≥ 3 independent experiments. Means \pm SEMs. *p < 0.05, **p < 0.01, and ***p < 0.001 by unpaired t test. See also Figure S2.

apparent immunosuppressive phenotype is associated with immunosuppressive functions. For this, we co-cultured naive CD4⁺ T cells derived from Foxp3^{GFP} mice with either Smad7^{fl/fl} or Smad7^{-/-} DCs in the presence or absence of TGF-β. We found that Smad7^{-/-} DCs induce enhanced differentiation of Foxp3⁺ Tregs, a difference that is further amplified by TGF-β (Figure 2D). We also found enhanced expression of the regulatory marker PD1 on T cells co-cultured with Smad7^{-/-} DCs (Figure 2E). To investigate whether the increased production of TGF-β alone may account for the ability of Smad7^{-/-} DCs to up-regulate Foxp3 in CD4⁺ T cells, we tested the ability of Smad7^{-/-} DCs to induce Foxp3 in the presence of the TGF-β-neutralizing antibody. Neutralizing TGF-β results in the partial abrogation of Foxp3 induction in CD4⁺ T cells, suggesting that an additional pathway may be involved (Figure 2F). We did not observe differences in Smad7^{fl/fl} DCs, which show minimal baseline Foxp3 induction under all treatment conditions (data not shown).

The PDL1/PD1 axis has been characterized as a potent inhibitor of immune activation, particularly through the inhibition of effector T cell function (Francisco et al., 2010). PD1 signaling has been shown to induce tolerance in part by promoting the development of Foxp3⁺ Tregs (Francisco et al., 2009). We thus asked whether the higher PDL1 and PDL2 expression by Smad7^{-/-} DCs, as well as the increased PD1 induction on T cells by Smad7^{-/-} DCs, serve as an additional signal to promote Foxp3⁺ Treg development. Although we found that blocking PD1 reduces Foxp3⁺ Tregs, the combination of both TGF-β-neutralizing and PD1-blocking antibodies synergistically reduces the Treg differentiation induced by Smad7^{-/-} DCs to the level induced by Smad7^{fl/fl} DCs (Figure 2F). Smad3^{-/-} DCs, which express reduced CD103, PD1 ligands, and TGF-β, are also defective in inducing Foxp3⁺ Tregs (Figure S2B). Correspondingly, enhanced Foxp3⁺ Treg induction by WT CD103⁺ DCs compared to CD103⁻ DCs is abrogated when co-cultured with PD1-deficient T cells (Figure 2G), suggesting that PD1 signaling also mediates CD103⁺ DC-induced Treg differentia-

tion. To further investigate the relative contribution of PDL1-PD1 and PDL2-PD1 signaling on Foxp3⁺ Treg cell development, we activated naive CD4⁺ T cells with or without TGF-β in the presence or absence of recombinant PDL1 and PDL2 Fc chimera proteins (PDL1-Fc and PDL2-Fc). The addition of either PDL1-Fc or PDL2-Fc without TGF-β (either added alone or with additional TGF-β-neutralizing antibody to address low levels of endogenous TGF-β) modestly promotes Tregs, but PDL1-Fc and PDL2-Fc greatly enhance Tregs induced by exogenous TGF-β (Figure 2H). These results suggest that Smad7 deficiency in DCs promotes TGF-β- and PDL2/1-mediated Treg differentiation.

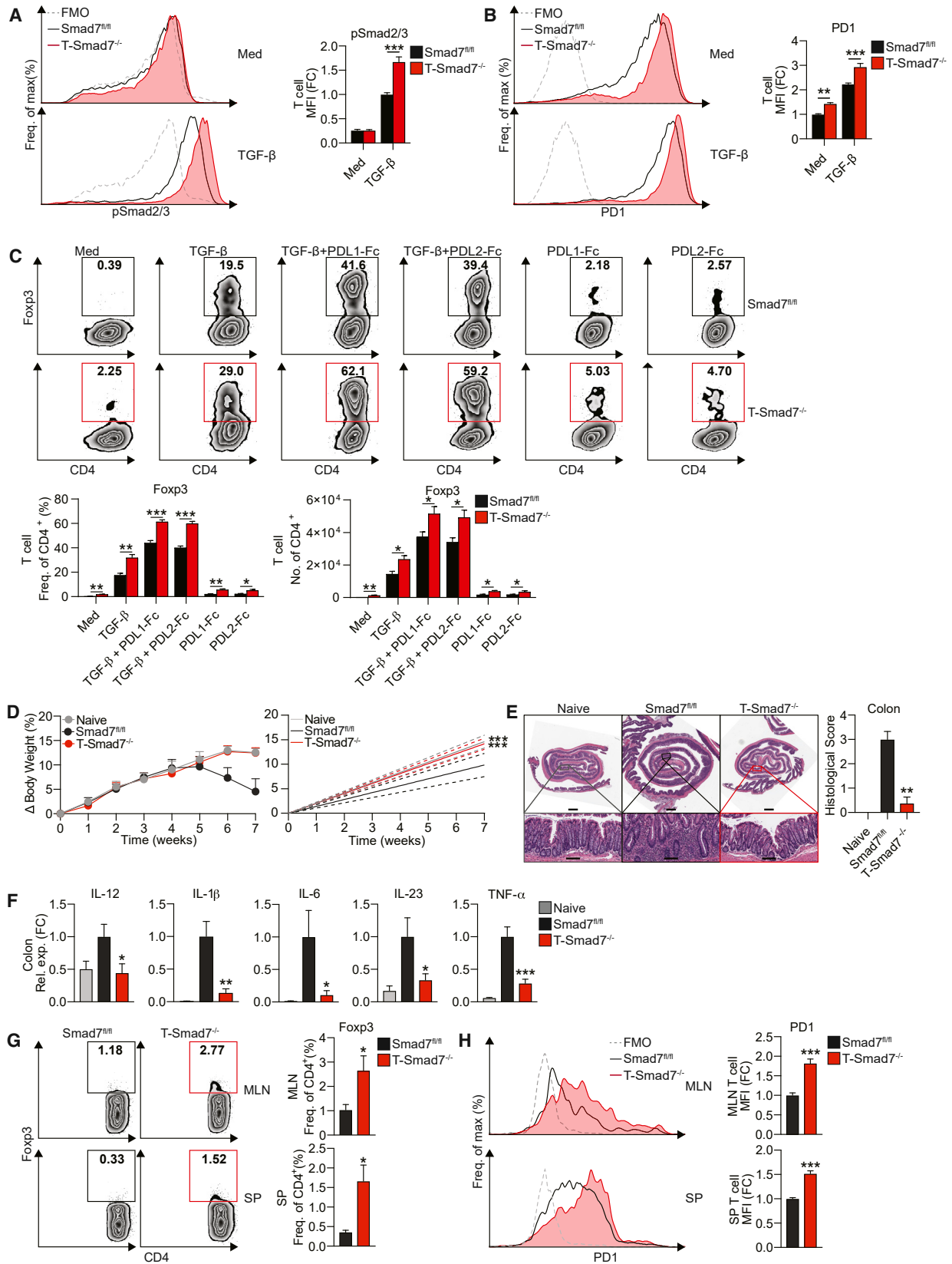
Smad7 Deletion in Dendritic Cells Reduces Colitis Severity in Mice

Smad7 has been reported to be increased in IBD patients (Monteleone et al., 2001, 2005). In parallel, we found Smad7 to be upregulated in immune cells in a DSS-induced colitis model (Figure S3A). Since we found that Smad7^{-/-} DCs demonstrate an enhanced ability to drive Treg differentiation, we asked whether Smad7 deficiency in DCs could protect mice from intestinal inflammation. Compared to Smad7^{fl/fl} mice, DC-Smad7^{-/-} mice given DSS lose significantly less weight (Figure 3A) and show a reduction in overall disease activity index, which accounts for the presence of blood in the stool and diarrhea in addition to weight changes (Figure 3B). DC-Smad7^{-/-} colons also display a significantly decreased histopathological score, as characterized by more intact crypt architecture and decreased inflammatory cell infiltration (Figure 3C). Furthermore, the pathological shortening of colon length was modestly less pronounced in colitic DC-Smad7^{-/-} mice (Figure 3D). To characterize differences in inflammatory signaling associated with colitis, we profiled the expression of inflammatory cytokines and chemokines in distal colon homogenates from colitic Smad7^{fl/fl} and DC-Smad7^{-/-} mice. Consistent with decreased inflammatory infiltrates, we found

Figure 3. Smad7 Deficiency in DCs Protects Mice against DSS-Induced Colitis

- (A) Percentage body weight changes (left) and linear regression analysis (right) of Smad7^{fl/fl} and DC-Smad7^{-/-} mice treated with 3% DSS in drinking water for 7 days (n = 8).
- (B) Disease activity index, a composite of body weight loss, blood in stool, and consistency of stool (higher score corresponds to colitis severity) (left) and linear regression analysis (right) of Smad7^{fl/fl} and DC-Smad7^{-/-} mice treated with 3% DSS in drinking water for 7 days (n = 9).
- (C) Representative histological sections with H&E (left) and scores (n = 10) (right) of colitic mice based on degree of ulceration at day 7, scored blinded by a pathologist at HRHCF. Scale bars represent ~1 mm (top) and ~100 μm (bottom).
- (D) Colon lengths of colitic mice at day 7 (n = 13).
- (E) Representative NanoString (immunology panel) heatmap of inflammatory and regulatory genes in distal colon from colitic Smad7^{fl/fl} and DC-Smad7^{-/-} mice. Important upregulated and downregulated genes of interest in DC-Smad7^{-/-} are highlighted in red and green, respectively.
- (F) qRT-PCR validation of selected genes, including IL-1β, IL-6, TNF-α, and IL-18 expression in these samples (n = 3).
- (G) qRT-PCR of TGF-β, CD103, IL-12, IL-1β, IL-6, IL-23, and TNF-α expression in MLN CD11c⁺ DCs from colitic mice (n = 5).
- (H) Representative FACS histograms (left) and MFIs (right) of PDL2, PDL1, and CD103 in MLN CD11c⁺ DCs from colitic mice (n = 3). MFI data reflective of CD11c⁺ population and expressed as FC from Smad7^{fl/fl} condition.
- (I) qRT-PCR of Foxp3, IFN-γ, and IL-17a in MLN CD4⁺ T cells (n = 5).
- (J) Representative FACS plots (left) and frequencies (right) of Foxp3⁺, IFN-γ⁺, and IL-17a⁺ populations in MLN (top) and lamina propria (LP) (bottom) CD4⁺ T cells (n = 4–10).
- (K) Percentage of body weight scores (left) and linear regression analyses (right) of Smad7^{fl/fl} and DC-Smad7^{-/-} mice treated during DSS administration, as indicated. Mice were treated with either immunoglobulin (Ig) control, (top) anti-CD25 (500 μg) (center), or anti-PD1 (250 μg) (bottom), given i.p. every other day 4 times, starting with DSS administration at day 0 (n = 3–4). Only control colitis body weight loss data for anti-CD25 are shown. Control data for anti-PD1 are identical (data not shown).

Data representative of ≥ 3 independent experiments. qRT-PCR data expressed as FC from Smad7^{fl/fl} condition. Means ± SEMs. *p < 0.05, **p < 0.01, ***p < 0.001 by unpaired t test. See also Figure S3.



(legend on next page)

reduced levels of proinflammatory mediators in DC-Smad7^{-/-} mice (Figure 3E). We then validated the expression of selected genes (interleukin 1 β [IL-1 β], IL-6, tumor necrosis factor α [TNF- α], and IL-18) known to play a key role in inflammation by qRT-PCR (Figure 3F) (Kaser et al., 2010). In addition, we found that MLN DCs from colitic DC-Smad7^{-/-} mice express higher levels of TGF- β and reduced levels of Th1- and Th17-polarizing cytokines (Figure 3G). We also found that increased TGF- β in Smad7^{-/-} DCs is associated with increased PDL2 and CD103 (Figures 3H). Although a previous report found altered indoleamine 2,3-dioxygenase (IDO) in Smad7^{-/-} DCs *in vivo* in other contexts (Lukas et al., 2017), we found no difference in IDO expression (data not shown). We also found no difference in retinoic acid (RA)-metabolizing enzymes in Smad7^{-/-} DCs during colitis (data not shown), which have been associated with CD103⁺ DCs (Coombes et al., 2007). To assess whether Smad7 deficiency in DCs has the capacity to modulate T cell cytokines *in vivo*, we measured these cytokines in colitic mice. CD4⁺ T cells from DC-Smad7^{-/-} mice express more Foxp3 and less interferon γ (IFN- γ) and IL-17a, both at mRNA (Figure 3I) and protein levels in the MLN and lamina propria (Figure 3J).

To further examine the contribution of Tregs and Treg-promoting PD1 signaling in mitigating colitis severity in DC-Smad7^{-/-} mice, colitic Smad7^{fl/fl} and DC-Smad7^{-/-} mice were treated with blocking antibodies to PD1 and CD25. We found that each blocking antibody is able to abrogate colitis resistance observed in control-treated DC-Smad7^{-/-} mice, indicating an indispensable role for Tregs and Treg-promoting PD1 signaling in mitigating colitis in DC-Smad7^{-/-} mice (Figure 3K). Experimental autoimmune encephalomyelitis (EAE), a mouse model for multiple sclerosis characterized by ascending paralysis, is another *in vivo* model in which DCs play an important role (Yogev et al., 2012). Similar to colitis, we found that DC-Smad7^{-/-} mice develop attenuated EAE and neuroinflammation (Figures S3B and S3C) associated with tolerogenic DC and T cell profiles, including increased Treg frequency (Figures S3D and S3E). Our data suggest that Smad7-deficiency in DCs exerts protective Treg-mediated effects during DSS-induced colitis and other autoimmune conditions.

Smad7 Restricts T Cell Responsiveness to TGF- β and PD1-Mediated Treg Differentiation and Promotes Colitis in a T Cell-Intrinsic Manner

Because we found that the enhanced ability of Smad7^{-/-} DCs to induce PD1 on CD4⁺ T cells (Figure 2E) is associated with increased TGF- β in Smad7^{-/-} DCs (Figure 2A), we tested the functional role of TGF- β on PD1 induction. The neutralization of TGF- β in DC-CD4⁺ T cell co-cultures mitigates enhanced PD1 induction on T cells by Smad7^{-/-} DCs (Figure S4A). We next stimulated naive CD4⁺ T cells in the presence or absence of TGF- β to directly assess the effect of TGF- β on PD1. Consistent with a recent report (Park et al., 2016), we found increased PD1 on CD4⁺ T cells stimulated with TGF- β (and activated with low-dose anti-CD3/28, which itself can induce PD1) (Figure S4B) (Nakae et al., 2006). Our TFBS analysis, followed by ChIP and luciferase assays, support that TGF- β transcriptionally activates the *Pdcd1* (PD1) promoter in T cells in a Smad3-dependent manner (Figures S4C–S4F). This is further confirmed by impaired PD1 induction in response to TGF- β in Smad3^{-/-} T cells (Figure S4G).

We and others have reported that in mouse and human T cells, TGF- β stimulation increases Smad7, which can inhibit TGF- β -induced Smad3 (Fantini et al., 2004; Murugaiyan et al., 2015). Therefore, to investigate whether Smad7 also limits TGF- β responsiveness and PD1 expression on CD4⁺ T cells, we generated mice deficient in Smad7 in CD4⁺ T cells (T-Smad7^{-/-}) (Figure S4H). We found that naive CD4⁺ T cells from T-Smad7^{-/-} mice show increased Smad2/3 phosphorylation (Figure 4A) associated with enhanced PD1 induction (Figure 4B), which corresponds to improved Treg differentiation in response to TGF- β and PDL1/2 stimulation *in vitro* (Figure 4C). Based on our observation that higher PD1 expression by Smad7^{-/-} CD4⁺ T cells favors Treg development *in vitro*, we asked whether the adoptive transfer of Smad7^{-/-} CD4⁺ T cells would result in reduced colitis severity in a T cell-mediated colitis model. Therefore, we transferred CD45RB^{hi}CD4⁺ T cells from Smad7^{fl/fl} and T-Smad7^{-/-} mice to Rag-1^{-/-} mice (Figure 4D). We found that Rag-1^{-/-} mice that receive CD4⁺ T cells from Smad7^{fl/fl} mice begin to lose weight in 5 weeks and develop severe colitis; however, mice that received CD4⁺ T cells from T-Smad7^{-/-} mice are protected (Figure 4D). We confirmed the development of colitis in

Figure 4. Smad7 Limits PD1 on CD4⁺ T Cells and PD1-Mediated Treg Differentiation and Promotes T Cell-Mediated Colitis

(A) Representative FACS histograms (left) and MFIs (right) of phospho-Smad2/3 in naive CD4⁺ T cells from Smad7^{fl/fl} and T-Smad7^{-/-} mice stimulated with or without TGF- β (2.5 ng/mL), for 1 h (n = 4). (B) Representative FACS histograms (left) and MFIs (right) of PD1 in naive CD4⁺ T cells from these mice stimulated with low-dose plate-bound anti-CD3/CD28 (1 μ g/mL) with or without TGF- β (2.5 ng/mL), for 18 h (n = 8). (C) Representative FACS plots (top), frequencies (bottom left), and cell counts per well (bottom right) of Foxp3⁺ populations in naive CD4⁺ T cells from these mice stimulated with or without TGF- β (0.5 ng/mL) and recombinant plate-bound PDL1-Fc or PDL2-Fc (30 μ g/mL), for 4 days (n = 5). (D–H) Colitis was induced by adoptive transfer of 6×10^5 CD4⁺CD45RB^{hi} T cells i.p. into Rag-1^{-/-} mice, followed by monitoring for 7 weeks. (D) Percentage body weight changes (left) and linear regression analysis (right) of Rag-1^{-/-} mice injected with CD4⁺CD45RB^{hi} T cells from Smad7^{fl/fl} or T-Smad7^{-/-} mice (n = 8). (E) Representative histological sections stained with H&E of distal colons (left) and histological scores (n = 8) (right) from recipient Rag-1^{-/-} mice, based on the degree of epithelial damage, as scored blinded by a pathologist at HRHCF. Scale bars represent \sim 1 mm (top) and \sim 100 μ m (bottom). (F) qRT-PCR of IL-12, IL-1 β , IL-6, IL-23, and TNF- α in colitic tissue from recipient mice (n = 8). (G) Representative FACS plots (left) and frequencies (right) of Foxp3⁺ populations in MLN (top) and splenic (bottom) CD4⁺ T cells from recipient mice at 7 weeks (n = 5–8). (H) Representative FACS histograms (left) and frequencies (right) of PD1 in MLN (top) and splenic (bottom) CD4⁺ T cells from recipient mice at 1 week (n = 6). Data representative of \geq 2 independent experiments. qRT-PCR and MFI (reflective of CD4⁺ population) data expressed as FC from Smad7^{fl/fl} media condition. Statistical comparisons to Smad7^{fl/fl} condition. *p < 0.05, **p < 0.01, and ***p < 0.001 by unpaired t test. See also Figures S4 and S5.

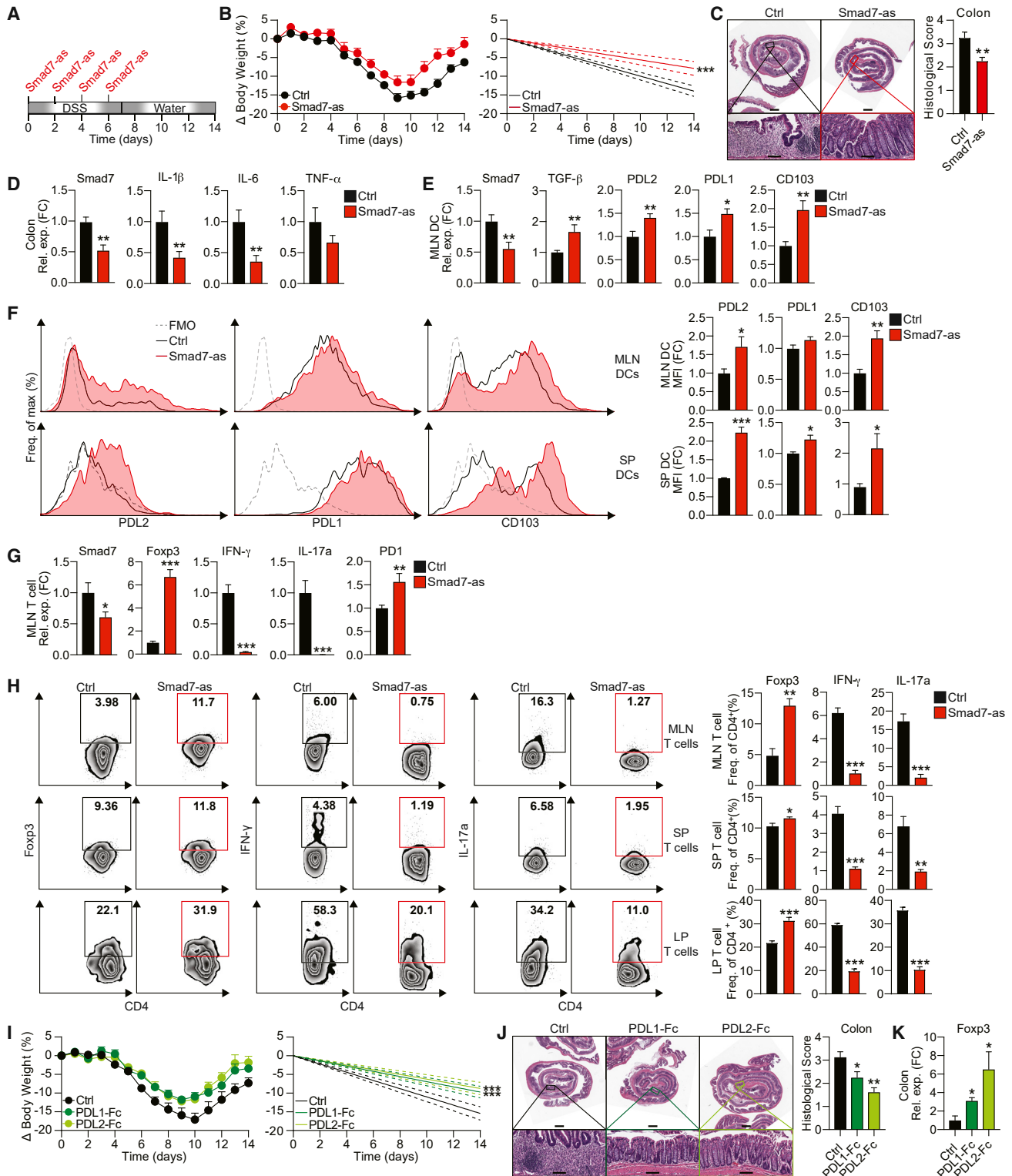


Figure 5. Smad7 Inhibition Ameliorates DSS-Induced Colitis in Mice

(A) Schematic of DSS colitis induction (3% DSS in water for 7 days, untreated drinking water for 7 days) and Smad7-as treatment i.p. (250 µg per mouse every other day 4 times).

(B) Percentage body weight changes (left) and linear regression analysis (right) of colitic mice treated with Smad7-as or its oligonucleotide control (n = 8).

(legend continued on next page)

mice reconstituted with Smad7^{fl/fl} CD4⁺ T cells by histological analysis at 7 weeks, which is characterized by marked inflammation (Figure 4E) and increased inflammatory cytokine expression in the colon (Figure 4F), both of which are significantly diminished in mice reconstituted with Smad7^{-/-} CD4⁺ T cells. We also found an increase in the fraction of Foxp3⁺ Tregs (Figure 4G) and PD1⁺ T cells (Figure 4H) in the MLNs and spleens of Smad7^{-/-} CD4⁺ T cell recipients. This is consistent with our *in vitro* data showing higher PD1 expression in Smad7^{-/-} T cells, which is associated with an increased ability to differentiate into Tregs in response to TGF- β and PDL2/1 stimulation (Figures 4B and 4C). In addition, we found that T-Smad7^{-/-} mice are less susceptible to DSS-induced colitis (Figures S5A and S5B), during which they also present with greater Treg frequency (Figure S5C). These results suggest that Smad7-deficiency in CD4⁺ T cells promotes PD1 upregulation and PD1-mediated Treg differentiation, conferring resistance to colonic inflammation.

Smad7 Inhibition Ameliorates DSS-Induced Colitis in Mice

Although TGF- β is highly expressed in IBD patients, TGF- β signaling is impaired due to high Smad7 activity (Monteleone et al., 2001). Accordingly, restoring TGF- β signaling with an anti-Smad7 oligonucleotide that specifically targets Smad7 mRNA has been effective in several inflammatory models (Boirivant et al., 2006; Kleiter et al., 2007) and in some CD (Feagan et al., 2018; Marafini et al., 2017; Monteleone et al., 2015) and UC patients in a recent trial (ClinicalTrials.gov: NCT02601300).

Our data suggest that the deletion of Smad7 in DCs (Figure 3) and T cells (Figure S5) protects mice from a DSS-induced UC model (Chassaing et al., 2014). Therefore, we investigated whether Smad7 inhibition using Smad7-antisense (Smad7-as) could also ameliorate this type of colitis in mice (Figure 5A). The same sequence Smad7-as inhibitor has previously been validated by others *in vitro* (Monteleone et al., 2001) and *in vivo* in models of CD and neuroinflammation (Boirivant et al., 2006; Kleiter et al., 2007) and in CD patients (Feagan et al., 2018; Monteleone et al., 2015). Two of these studies have demonstrated Smad7-as to be effectively uptaken by immune cells in the periphery and gut (Boirivant et al., 2006; Kleiter et al., 2007). In agreement with these studies, we found that the administration of Smad7-as during DSS-induced colitis ameliorates disease. Smad7-as-treated mice lose less weight (Figure 5B) and show

less colonic inflammation (Figure 5C), which is associated with decreased expression of Smad7 and inflammatory genes in the colon (Figure 5D). Furthermore, MLN DCs from Smad7-as-treated mice express decreased Smad7, indicating that Smad7-as effectively inhibits Smad7 in these cells, along with increased TGF- β (Figure 5E). Consistent with elevated TGF- β , we found enhanced PDL2, PDL1, and CD103 both at mRNA (Figure 5E) and protein levels (Figure 5F). In addition, Smad7-as-treated mice exhibit decreased Smad7 in T cells, demonstrating Smad7-as efficacy in these cells, alongside higher levels of Foxp3 and PD1 and reduced IFN- γ and IL-17a at the mRNA level (Figure 5G). Correspondingly, increased frequencies of Foxp3⁺ Tregs and reduced frequencies of IFN- γ - and IL-17a-producing CD4⁺ T cells are observed in Smad7-as-treated mice (Figure 5H). These data suggest that Smad7 inhibition ameliorates a model of UC, which may be mediated via the tolerogenic effects of Smad7 suppression in DCs and CD4⁺ T cells.

Because we observed that Smad7 inhibition in DSS-induced colitis is associated with the enhancement of PDL2/1 in DCs and of PD1 in CD4⁺ T cells, we tested whether agonizing PD1 directly via PDL2-Fc and PDL1-Fc would ameliorate colitis. We found that the preclinical treatment of mice significantly ameliorates colitis and enhances recovery as determined by reduced body weight loss (Figure 5I) and decreased colonic inflammation (Figure 5J). This colitis mitigation in PDL2-Fc- or PDL1-Fc-treated mice is associated with increased colonic Foxp3 expression (Figure 5K). These data further implicate PDL2/1 signaling in suppressing colitis and demonstrate that directly enhancing PDL2/1-PD1 signaling therapeutically through the administration of PDL2/1-Fc can ameliorate a mouse model of UC.

DISCUSSION

Smad7 is one of the proteins that has been heavily implicated in immune dysregulation during IBDs. In fact, elevated colonic Smad7 has been associated with enhanced inflammation in IBD patients (Monteleone et al., 2001, 2005). Several factors could contribute to this increase in Smad7, including IL-1 β , TNF- α , IFN- γ , and TGF- β (Monteleone et al., 2001). However, the exact molecular pathways by which Smad7 mediates its pathogenic functions in IBDs, including its cell type-specific functions, have not been determined. Here, we have identified critical cell populations and mechanisms underlying pathogenic Smad7 functions in

(C) Representative histopathological sections with H&E (left) and scores (n = 8) (right) based on the degree of ulceration at day 14, scored blinded by a pathologist at HRHCF. Scale bars represent ~1 mm (top) and ~100 μ m (bottom).

(D) qRT-PCR of Smad7, IL-1 β , IL-6, and TNF- α expression in colitic tissue (n = 10–15).

(E) qRT-PCR of Smad7, TGF- β , PDL2, PDL1, and CD103 expression in MLN CD11c⁺ DCs from colitic mice (n = 10).

(F) Representative FACS histograms (left) and MFIs (right) of PDL2, PDL1, and CD103 in MLN (top) and splenic (bottom) CD11c⁺ DCs from colitic mice (n = 5–10). MFI data reflective of CD11c⁺ population and expressed as FC from control condition.

(G) qRT-PCR of Smad7, Foxp3, IFN- γ , IL-17a, and PD1 expression in CD4⁺ MLN T cells (n = 5–10).

(H) Representative FACS plots (left) and frequencies (right) of Foxp3⁺, IFN- γ ⁺, and IL-17a⁺ populations in CD4⁺ MLN (top), splenic (center), and LP (bottom) T cells (n = 4–5).

(I–K) DSS colitis was induced (3% DSS in water for 7 days, untreated drinking water for 7 days) and PDL1-fc or PDL2-fc treatment were given i.p. (100 μ g per mouse every other day 4 times) as in (A). (I) Percentage body weight changes (left) and linear regression analysis (right) of colitic mice treated with PDL1-Fc, PDL2-Fc, or Ig control (n = 5–7). (J) Representative histopathological sections (left) and scores (right) based on the degree of ulceration, scored blinded by a pathologist at HRHCF (n = 8). Scale bars represent ~1 mm (top) and ~100 μ m (bottom). (K) qRT-PCR of Foxp3 expression in colitic tissue (n = 4–5).

Data representative of ≥ 3 independent experiments. qRT-PCR and MFI data expressed as FC from control condition. Means \pm SEMs. *p < 0.05, **p < 0.01, and ***p < 0.001 by unpaired t test.

colitis. Specifically, by using DC- and CD4⁺ T cell-specific Smad7-knockout mice, we have uncovered that Smad7 mediates intestinal inflammation by limiting PDL2/1-PD1 signaling, a major immunoregulatory axis in Treg differentiation and immune tolerance.

The PD1-PDL1 pathway plays a critical role in peripheral tolerance to protect against autoimmunity (Francisco et al., 2010). There is also considerable evidence that PDL2 inhibits lymphocyte activation by binding to PD1 (Zhang et al., 2006). Decreased PDL1 expression in intestinal APCs has been observed in IBD patients, and blocking PDL1 signaling has been found to promote intestinal inflammation both in mice and humans (Bertha et al., 2017; Reynoso et al., 2009; Robertson et al., 2016; Scanduzzi et al., 2014; Wang et al., 2017). However, the role of PDL2 and the regulatory mechanisms that control PDL2-PD1 signaling in IBDs remain unclear. Our data demonstrate that Smad7 sustains detrimental immune responses in IBDs by inhibiting the PDL2/1-PD1 pathway via action within DCs and CD4⁺ T cells.

While CD103⁻ intestinal DCs promote colitogenic immune responses in colitis, CD103⁺ DCs maintain intestinal homeostasis (Kourepini et al., 2014). Altered CD103⁺ DC frequencies have been observed in colitis patients and animal models (Kourepini et al., 2014; Matsuno et al., 2017; Wenzel et al., 2014). In fact, specific deletion of CD103⁺ DCs worsens colitis in mice (Muzaki et al., 2016). However, the molecular pathways that prevent the development of intestinal CD103⁺ DCs in IBDs remain unclear. Although TGF- β R and Smad7 deficiency are known to alter regulatory DCs (Bain et al., 2017; Lukas et al., 2017), our study has identified Smad7 as a key player in this process that limits the generation of PDL1⁻, PDL2⁻, and CD103-expressing regulatory DCs. Specifically, we describe how Smad7 restrains a TGF- β -mediated transcriptional program via Smad3. While our present findings establish that genetic deletion or pharmacological inhibition of Smad7 is of therapeutic value in colitis by enhancing CD103 and PD1 ligands on DCs, it remains to be explored which factors control Smad7 levels and govern this process in CD103⁻ and CD103⁺ DCs during disease. Emerging studies suggest that several inflammatory cytokines, such as TNF- α and IL-1 β , which are highly expressed by CD103⁻ DCs (Coombes et al., 2007; Ruane and Lavelle, 2011), can limit the conversion to CD103⁺ DCs in the gut (Mak'Anyengo et al., 2018) while inducing Smad7 (Baugé et al., 2008). Therefore, CD103⁻ DCs secreting these inflammatory cytokines may inherently upregulate Smad7 in an autocrine manner and become less responsive to TGF- β , which in turn could result in less PD1 ligand and CD103 expression by these DCs. A better understanding of this process could present alternative avenues for therapeutically manipulating Smad7 signaling in intestinal inflammation.

One of the major mechanisms by which intestinal CD103⁺ DCs mediate their protective functions in colitis is by inducing Tregs (Jaensson et al., 2008). Several context-dependent pathways have been linked to this specialization for Treg differentiation. CD103⁺ DCs have been shown to express higher levels of TGF- β and promote Treg differentiation, which is further enhanced by exogenous TGF- β . In addition to increased TGF- β secretion, intestinal CD103⁺ DCs have been shown to express more RA-metabolizing enzymes. The addition of exogenous TGF- β along with RA further promotes Treg differentiation (Coombes et al., 2007). However, a dispensable role for RA in

CD103⁺ DCs in Treg development also exists (Worthington et al., 2011). We found no difference in RA-metabolizing enzymes in Smad7^{-/-} DCs during colitis, suggesting that Smad7^{-/-} DCs leverage RA-independent pathways in promoting Tregs. Another role forIDO-mediated Treg differentiation specifically in Smad7-deficient CD103⁺ DCs has been described in EAE (Lukas et al., 2017).IDO is strongly induced by IFN- γ (Jürgens et al., 2009), which permeates the CNS microenvironment during EAE due to a higher load of infiltrating IFN- γ -secreting Th1 cells (Fletcher et al., 2010). We found no difference in IDO in Smad7^{-/-} DCs in colitis, implicating other pathways in promoting Tregs, such as PDL2/1-PD1 signaling, as demonstrated by our *in vitro* and *in vivo* profiling and rescue data. We found that CD103⁺ DCs express higher levels of PDL2 and a moderate increase in PDL1 (possibly reflecting already high baseline PDL1 expression) on their surface compared to CD103⁻ DCs. Moreover, we revealed that preventing PDL2/1-PD1 interaction abrogates Treg induction by CD103⁺ DCs. Consistent with this, others have found that CD103⁺ DCs from tumor-draining lymph nodes express more PDL1 and contribute to immunosuppression (Salmon et al., 2016). Although PDL1 has been linked to Treg induction, we have identified a role for PDL2 in Treg differentiation and the potentially greater significance of PDL2 versus PDL1 in this context, based on the stronger association of PDL2 with CD103⁺ and Smad7^{-/-} DCs.

Although PD1-blocking antibodies have transformed the management and prognosis of cancer patients, PD1 blockade-induced colitis is an increasingly recognized immune-related adverse event that shares many characteristics with IBDs, demonstrating the importance of an intact PDL2/1-PD1 axis in intestinal immune tolerance (Bertha et al., 2017; Wang et al., 2017). However, the molecular mechanisms that control the expression of PD1 during IBDs remain poorly understood. TGF- β and Smad7 deficiency are known to promote Treg development (Chen et al., 2003; Chen and Wahl, 2003; Kleiter et al., 2010). Here, we have identified a T cell-intrinsic mechanism whereby the Smad7-mediated regulation of PD1 underlies this effect on Treg differentiation, a process that is deeply intertwined with Smad7 regulation of PDL2/1 in DCs. Consistent with a recent report (Park et al., 2016), we found that TGF- β transcriptionally promotes PD1 on T cells in a Smad3-dependent manner, which is enhanced in the absence of Smad7. The adoptive transfer of Smad7-deficient CD4⁺ T cells confers protection against a T cell-mediated colitis model and appears to be mediated by increased PD1-mediated Treg differentiation *in vivo*. CD4⁺ Treg induction and colitis attenuation are also observed in DSS colitis in T-Smad7^{-/-} mice. Although colonic CD8⁺ T cells are less abundant than CD4⁺ T cells in DSS colitis (Shale et al., 2013), PD1 on CD8⁺ T cells could be affected by Smad7 deletion (due to double CD4⁺CD8⁺ stage during thymic development) and remains to be investigated.

Elevated Smad7 has been associated with sustained inflammation in IBDs and other chronic inflammatory disorders (Kleiter et al., 2007; Monteleone et al., 2001). Antisense Smad7 oligonucleotide that specifically targets SMAD7 mRNA has been effective in patients with CD in multiple independent phase II trials (Feagan et al., 2018; Marafini et al., 2017; Monteleone et al., 2015), as well as in an IBD model (Boirivant et al., 2006). In

addition, Smad7 silencing has been shown to resolve inflammation in a model of CNS autoimmunity in mice (Kleiter et al., 2007). Recently, a phase III trial with the Smad7 inhibitor Mongersen in CD was discontinued following an interim futility report despite multiple independent positive phase II results (Feagan et al., 2018; Lowe, 2017; Marafini et al., 2017; Monteleone et al., 2015). Details for this discrepancy remain unclear. The lack of clear markers of target engagement, the oral route of administration of the antisense oligonucleotide, and dose-finding based on extrapolation from preclinical models may have contributed. However, a phase II trial with the same Smad7-as in UC has shown modest success in a single-arm open-label study as measured by clinical response and endoscopic remission (ClinicalTrials.gov: NCT02601300). Our results demonstrate that the specific deletion of Smad7 in DCs and T cells protects mice from a model of DSS-induced colitis resembling UC (Chassaing et al., 2014). Correspondingly, we found that Smad7-as treatment given intraperitoneally (i.p.) ameliorates DSS colitis severity, suggesting that Smad7 inhibition could be more effective in UC patients if better targeted toward these immune cells. Our promising preclinical colitis data, combined with positive safety data across all Mongersen trials, provide justification for Smad7 inhibition efficacy to be further explored. We also provide evidence complementing other reports that Smad7 inhibition ameliorates EAE (Kleiter et al., 2010; Lukas et al., 2017), which may justify consideration of this therapy in other autoimmune conditions.

In addition, our deeper understanding of Smad7 networks has identified other pathways that could be targeted against intestinal inflammation. Here, we found that Smad7 deficiency in DCs and T cells is associated with increased PDL2/1-PD1 signaling and resistance to colitis in mice. Consistent with a previous report, which only explored PDL1 (Song et al., 2015), we also show the direct functional role of PDL2/1-PD1 signaling in colitis. Enhancing PD1 signaling via administration of Fc-fused PDL1 and PDL2 is effective in reducing DSS-induced colitis severity. These data raise the self-evident prospect that direct PDL2/1 modulation may be beneficial in IBD patients. This could be pursued independent of Smad7 inhibition therapy or in combination with Smad7 inhibition. Based on our data demonstrating that Smad7 antisense increases PD1 expression on T cells, Smad7 inhibition could synergistically enhance the sensitivity to tolerogenic signals from PDL2/1-Fc or similar molecules. Our data also suggest the possibility that Smad7 inhibition therapy may be more effective in patients with defective or decreased PD1 signaling, as we found that Smad7 therapy appears to mitigate the disease severity in preclinical colitis models via the upregulation of this pathway. Such PD1 differences in patients have been shown to modulate PD1-mediated therapeutic responses in cancer (Zou et al., 2016). Underscoring the importance of properly identifying IBD patient populations for Smad7-as therapy, a recent study suggests that expression of the chemokine CCL20 in CD patients predicts the response to Mongersen (Marafini et al., 2017). PD1 and its ligands may also be explored as a biomarker for predicting the efficacy of Smad7 inhibition therapy in UC. Our data also raise the prospect of Smad7 inhibition efficacy in inflammation-driven colorectal cancer, especially considering work showing a pathogenic role for Smad7 in regu-

lating the cell cycle in some intestinal cancer models (Halder et al., 2008; Stolfi et al., 2014). However, the relation between Smad7, PD1 signaling, and colorectal cancer remains unclear, as suggested by mixed results with PD1 inhibitors in colon cancer patients (Kalyan et al., 2018; Topalian et al., 2012) and Smad7 function in colon cancer models (Troncone and Monteleone, 2019). In summary, the present study identifies critical cell populations and mechanisms underlying pathogenic Smad7 function in IBDs and provides insights on the PDL2/1-PD1 axis and potential avenues for the therapeutic management of IBDs.

STAR★METHODS

Detailed methods are provided in the online version of this paper and include the following:

- KEY RESOURCES TABLE
- LEAD CONTACT AND MATERIALS AVAILABILITY
- EXPERIMENTAL MODEL AND SUBJECT DETAILS
 - Mice
- METHOD DETAILS
 - DSS-induced colitis
 - Smad7-as and PDL1/2-Fc treatment of colitis
 - CD4⁺CD45RB^{hi} T cell transfer colitis
 - EAE
 - Generation and isolation of DCs and T cells
 - TGF-β ELISA
 - DC-T cell co-culture
 - T cell culture
 - RNA isolation, cDNA synthesis, and quantitative Real-Time PCR
 - NanoString
 - Promoter analysis
 - ChIP assays
 - Luciferase assays
 - b. Secrete pair Gaussia Luciferase (GLuc) assay (Genecopoeia, Rockville, MD)
- QUANTIFICATION AND STATISTICAL ANALYSIS
 - Statistics
- DATA AND CODE AVAILABILITY

SUPPLEMENTAL INFORMATION

Supplemental Information can be found online at <https://doi.org/10.1016/j.celrep.2019.07.065>.

ACKNOWLEDGMENTS

We thank Dr. Lillian Maggio-Price (University of Washington, Seattle) for Smad3^{-/-} mice and Dr. Matthias Brock (University Hospital Zurich, Switzerland) for the pCMV6, pCMV6 SMAD3, and pRL-GAPDH constructs. This study was supported by the NIH (R01AI127853 to G.M.) and the National Multiple Sclerosis Society (RG 1507-05164 to G.M.).

AUTHOR CONTRIBUTIONS

L.P.G. and G.M. designed and performed experiments and analyzed data. A.K.A. performed ChIP and luciferase assays. M.F., V.B., C.K., G.G., S.S., R.R., and S.R. performed experiments. L.P.G. and G.M. prepared the manuscript, with participation from A.K.A., M.F., V.B., G.G., R.R., and H.L.W.

DECLARATION OF INTERESTS

The authors declare no competing interests.

Received: October 23, 2018

Revised: June 9, 2019

Accepted: July 18, 2019

Published: September 24, 2019

REFERENCES

- Afrakhte, M., Morén, A., Jossan, S., Itoh, S., Sampath, K., Westermarck, B., Heldin, C.H., Heldin, N.E., and ten Dijke, P. (1998). Induction of inhibitory Smad6 and Smad7 mRNA by TGF-beta family members. *Biochem. Biophys. Res. Commun.* **249**, 505–511.
- Ajay, A.K., Kim, T.M., Ramirez-Gonzalez, V., Park, P.J., Frank, D.A., and Vaidya, V.S. (2014). A bioinformatics approach identifies signal transducer and activator of transcription-3 and checkpoint kinase 1 as upstream regulators of kidney injury molecule-1 after kidney injury. *J. Am. Soc. Nephrol.* **25**, 105–118.
- Bain, C.C., Montgomery, J., Scott, C.L., Kel, J.M., Girard-Madoux, M.J.H., Martens, L., Zangerle-Murray, T.F.P., Ober-Biöbaum, J., Lindenbergh-Kortleve, D., Samsom, J.N., et al. (2017). TGFβR signalling controls CD103⁺CD11b⁺ dendritic cell development in the intestine. *Nat. Commun.* **8**, 620.
- Baugé, C., Attia, J., Leclercq, S., Pujol, J.P., Galéra, P., and Boumédiène, K. (2008). Interleukin-1beta up-regulation of Smad7 via NF-kappaB activation in human chondrocytes. *Arthritis Rheum.* **58**, 221–226.
- Bertha, M., Bellaguara, E., Kuzel, T., and Hanauer, S. (2017). Checkpoint Inhibitor-Induced Colitis: A New Type of Inflammatory Bowel Disease? *ACG Case Rep. J.* **4**, e112.
- Boden, E.K., and Snapper, S.B. (2008). Regulatory T cells in inflammatory bowel disease. *Curr. Opin. Gastroenterol.* **24**, 733–741.
- Boirivant, M., Pallone, F., Di Giacinto, C., Fina, D., Monteleone, I., Marinaro, M., Caruso, R., Colantoni, A., Palmieri, G., Sanchez, M., et al. (2006). Inhibition of Smad7 with a specific antisense oligonucleotide facilitates TGF-beta1-mediated suppression of colitis. *Gastroenterology* **131**, 1786–1798.
- Bouché, M., Canipari, R., Melchionna, R., Willems, D., Senni, M.I., and Molinaro, M. (2000). TGF-beta autocrine loop regulates cell growth and myogenic differentiation in human rhabdomyosarcoma cells. *FASEB J.* **14**, 1147–1158.
- Chassaing, B., Aitken, J.D., Malleshappa, M., and Vijay-Kumar, M. (2014). Dextran sulfate sodium (DSS)-induced colitis in mice. *Curr. Protoc. Immunol.* **104**, 25.
- Chen, W., and Wahl, S.M. (2003). TGF-beta: the missing link in CD4+CD25+ regulatory T cell-mediated immunosuppression. *Cytokine Growth Factor Rev.* **14**, 85–89.
- Chen, W., Jin, W., Hardegen, N., Lei, K.J., Li, L., Marinos, N., McGrady, G., and Wahl, S.M. (2003). Conversion of peripheral CD4+CD25- naive T cells to CD4+CD25+ regulatory T cells by TGF-beta induction of transcription factor Foxp3. *J. Exp. Med.* **198**, 1875–1886.
- Coombes, J.L., Siddiqui, K.R., Arancibia-Cárcamo, C.V., Hall, J., Sun, C.M., Belkaid, Y., and Powrie, F. (2007). A functionally specialized population of mucosal CD103+ DCs induces Foxp3+ regulatory T cells via a TGF-beta and retinoic acid-dependent mechanism. *J. Exp. Med.* **204**, 1757–1764.
- Dalal, S.R., and Chang, E.B. (2014). The microbial basis of inflammatory bowel diseases. *J. Clin. Invest.* **124**, 4190–4196.
- David, B.A., Rubino, S., Moreira, T.G., Freitas-Lopes, M.A., Araújo, A.M., Paul, N.E., Rezende, R.M., and Menezes, G.B. (2017). Isolation and high-dimensional phenotyping of gastrointestinal immune cells. *Immunology* **151**, 56–70.
- Eastaff-Leung, N., Mabarrack, N., Barbour, A., Cummins, A., and Barry, S. (2010). Foxp3+ regulatory T cells, Th17 effector cells, and cytokine environment in inflammatory bowel disease. *J. Clin. Immunol.* **30**, 80–89.
- Fantini, M.C., Becker, C., Monteleone, G., Pallone, F., Galle, P.R., and Neurath, M.F. (2004). Cutting edge: TGF-beta induces a regulatory phenotype in CD4+CD25- T cells through Foxp3 induction and down-regulation of Smad7. *J. Immunol.* **172**, 5149–5153.
- Farré, D., Roset, R., Huerta, M., Adsuara, J.E., Roselló, L., Albà, M.M., and Messeguer, X. (2003). Identification of patterns in biological sequences at the ALGGEN server: PROMO and MALGEN. *Nucleic Acids Res.* **31**, 3651–3653.
- Feagan, B.G., Sands, B.E., Rossiter, G., Li, X., Usiskin, K., Zhan, X., and Colombel, J.F. (2018). Effects of Mongersen (GED-0301) on Endoscopic and Clinical Outcomes in Patients With Active Crohn's Disease. *Gastroenterology* **154**, 61–64.e6.
- Fife, B.T., and Bluestone, J.A. (2008). Control of peripheral T-cell tolerance and autoimmunity via the CTLA-4 and PD-1 pathways. *Immunol. Rev.* **224**, 166–182.
- Fletcher, J.M., Lalor, S.J., Sweeney, C.M., Tubridy, N., and Mills, K.H. (2010). T cells in multiple sclerosis and experimental autoimmune encephalomyelitis. *Clin. Exp. Immunol.* **162**, 1–11.
- Francisco, L.M., Salinas, V.H., Brown, K.E., Vanguri, V.K., Freeman, G.J., Kuchroo, V.K., and Sharpe, A.H. (2009). PD-L1 regulates the development, maintenance, and function of induced regulatory T cells. *J. Exp. Med.* **206**, 3015–3029.
- Francisco, L.M., Sage, P.T., and Sharpe, A.H. (2010). The PD-1 pathway in tolerance and autoimmunity. *Immunol. Rev.* **236**, 219–242.
- Halder, S.K., Rachakonda, G., Deane, N.G., and Datta, P.K. (2008). Smad7 induces hepatic metastasis in colorectal cancer. *Br. J. Cancer* **99**, 957–965.
- Harrison, O.J., and Powrie, F.M. (2013). Regulatory T cells and immune tolerance in the intestine. *Cold Spring Harb. Perspect. Biol.* **5**, a018341.
- Izcue, A., Coombes, J.L., and Powrie, F. (2009). Regulatory lymphocytes and intestinal inflammation. *Annu. Rev. Immunol.* **27**, 313–338.
- Jaensson, E., Uronen-Hansson, H., Pabst, O., Eksteen, B., Tian, J., Coombes, J.L., Berg, P.L., Davidsson, T., Powrie, F., Johansson-Lindbom, B., and Agace, W.W. (2008). Small intestinal CD103+ dendritic cells display unique functional properties that are conserved between mice and humans. *J. Exp. Med.* **205**, 2139–2149.
- Jürgens, B., Hainz, U., Fuchs, D., Felzmann, T., and Heitger, A. (2009). Interferon-gamma-triggered indoleamine 2,3-dioxygenase competence in human monocyte-derived dendritic cells induces regulatory activity in allogeneic T cells. *Blood* **114**, 3235–3243.
- Kalyan, A., Kircher, S., Shah, H., Mulcahy, M., and Benson, A. (2018). Updates on immunotherapy for colorectal cancer. *J. Gastrointest. Oncol.* **9**, 160–169.
- Kaser, A., Zeissig, S., and Blumberg, R.S. (2010). Inflammatory bowel disease. *Annu. Rev. Immunol.* **28**, 573–621.
- Kashiwagi, I., Morita, R., Schichita, T., Komai, K., Saeki, K., Matsumoto, M., Takeda, K., Nomura, M., Hayashi, A., Kanai, T., and Yoshimura, A. (2015). Smad2 and Smad3 Inversely Regulate TGF-β Autoinduction in Clostridium butyricum-Activated Dendritic Cells. *Immunity* **43**, 65–79.
- Kim, J.J., Shajib, M.S., Manocha, M.M., and Khan, W.I. (2012). Investigating intestinal inflammation in DSS-induced model of IBD. *J. Vis. Exp.* (60), 3678.
- Kleiter, I., Pedré, X., Mueller, A.M., Poeschl, P., Couillard-Despres, S., Spruss, T., Bogdahn, U., Giegerich, G., and Steinbrecher, A. (2007). Inhibition of Smad7, a negative regulator of TGF-beta signaling, suppresses autoimmune encephalomyelitis. *J. Neuroimmunol.* **187**, 61–73.
- Kleiter, I., Song, J., Lukas, D., Hasan, M., Neumann, B., Croxford, A.L., Pedré, X., Hövelmeyer, N., Yögev, N., Mildner, A., et al. (2010). Smad7 in T cells drives T helper 1 responses in multiple sclerosis and experimental autoimmune encephalomyelitis. *Brain* **133**, 1067–1081.
- Kourepini, E., Aggelakopoulou, M., Alissafi, T., Paschalidis, N., Simoes, D.C., and Panoutsakopoulou, V. (2014). Osteopontin expression by CD103-dendritic cells drives intestinal inflammation. *Proc. Natl. Acad. Sci. USA* **111**, E856–E865.
- Liu, H., Bakthavatsalam, R., Meng, Z., Li, Z., Li, W., Perkins, J.D., and Reyes, J. (2013). PD-L1 signal on liver dendritic cells is critical for Foxp3(+)/CD4(+)/CD25(+) Treg and liver tolerance induction in mice. *Transplant. Proc.* **45**, 1853–1855.

- Lowe, D. (2017). *Mongersen Fails*. <https://blogs.sciencemag.org/pipeline/archives/2017/10/23/mongersen-fails>.
- Lukas, D., Yogeve, N., Kel, J.M., Regen, T., Mufazalov, I.A., Tang, Y., Wanke, F., Reizis, B., Müller, W., Kurschus, F.C., et al. (2017). TGF- β inhibitor Smad7 regulates dendritic cell-induced autoimmunity. *Proc. Natl. Acad. Sci. USA* *114*, E1480–E1489.
- Mak'Anyengo, R., Duewell, P., Reichl, C., Hörth, C., Lehr, H.A., Fischer, S., Clavel, T., Denk, G., Hohenester, S., Kobold, S., et al. (2018). Nlrp3-dependent IL-1 β inhibits CD103+ dendritic cell differentiation in the gut. *JCI Insight* *3*, 96322.
- Manicassamy, S., and Pulendran, B. (2011). Dendritic cell control of tolerogenic responses. *Immunol. Rev.* *241*, 206–227.
- Marafini, I., Monteleone, I., Dinallo, V., Di Fusco, D., De Simone, V., Laudisi, F., Fantini, M.C., Di Sabatino, A., Pallone, F., and Monteleone, G. (2017). CCL20 Is Negatively Regulated by TGF- β 1 in Intestinal Epithelial Cells and Reduced in Crohn's Disease Patients With a Successful Response to Mongersen, a Smad7 Antisense Oligonucleotide. *J. Crohn's Colitis* *11*, 603–609.
- Matsuno, H., Kayama, H., Nishimura, J., Sekido, Y., Osawa, H., Barman, S., Ogino, T., Takahashi, H., Haraguchi, N., Hata, T., et al. (2017). CD103+ Dendritic Cell Function Is Altered in the Colons of Patients with Ulcerative Colitis. *Inflamm. Bowel Dis.* *23*, 1524–1534.
- Messeguer, X., Escudero, R., Farré, D., Núñez, O., Martínez, J., and Albà, M.M. (2002). PROMO: detection of known transcription regulatory elements using species-tailored searches. *Bioinformatics* *18*, 333–334.
- Monteleone, G., Kumberova, A., Croft, N.M., McKenzie, C., Steer, H.W., and MacDonald, T.T. (2001). Blocking Smad7 restores TGF-beta1 signaling in chronic inflammatory bowel disease. *J. Clin. Invest.* *108*, 601–609.
- Monteleone, G., Del Vecchio Blanco, G., Monteleone, I., Fina, D., Caruso, R., Gioia, V., Ballerini, S., Federici, G., Bernardini, S., Pallone, F., and MacDonald, T.T. (2005). Post-transcriptional regulation of Smad7 in the gut of patients with inflammatory bowel disease. *Gastroenterology* *129*, 1420–1429.
- Monteleone, G., Neurath, M.F., Ardizzone, S., Di Sabatino, A., Fantini, M.C., Castiglione, F., Scribano, M.L., Armuzzi, A., Caprioli, F., Sturniolo, G.C., et al. (2015). Mongersen, an oral SMAD7 antisense oligonucleotide, and Crohn's disease. *N. Engl. J. Med.* *372*, 1104–1113.
- Murugaiyan, G., da Cunha, A.P., Ajay, A.K., Joller, N., Garo, L.P., Kumaradevan, S., Yosef, N., Vaidya, V.S., and Weiner, H.L. (2015). MicroRNA-21 promotes Th17 differentiation and mediates experimental autoimmune encephalomyelitis. *J. Clin. Invest.* *125*, 1069–1080.
- Muzaki, A.R., Tettak, P., Sheng, J., Loh, S.C., Setiagani, Y.A., Poidinger, M., Zolezzi, F., Karjalainen, K., and Ruedl, C. (2016). Intestinal CD103(+) CD11b(-) dendritic cells restrain colitis via IFN- γ -induced anti-inflammatory response in epithelial cells. *Mucosal Immunol.* *9*, 336–351.
- Nakae, S., Suto, H., Iikura, M., Kakurai, M., Sedgwick, J.D., Tsai, M., and Galli, S.J. (2006). Mast cells enhance T cell activation: importance of mast cell costimulatory molecules and secreted TNF. *J. Immunol.* *176*, 2238–2248.
- Park, B.V., Freeman, Z.T., Ghasemzadeh, A., Chattergoon, M.A., Rutebemberwa, A., Steigner, J., Winter, M.E., Huynh, T.V., Sebald, S.M., Lee, S.J., et al. (2016). TGF β 1-Mediated SMAD3 Enhances PD-1 Expression on Antigen-Specific T Cells in Cancer. *Cancer Discov.* *6*, 1366–1381.
- Rescigno, M., and Di Sabatino, A. (2009). Dendritic cells in intestinal homeostasis and disease. *J. Clin. Invest.* *119*, 2441–2450.
- Reynoso, E.D., Elpek, K.G., Francisco, L., Bronson, R., Bellemare-Pelletier, A., Sharpe, A.H., Freeman, G.J., and Turley, S.J. (2009). Intestinal tolerance is converted to autoimmune enteritis upon PD-1 ligand blockade. *J. Immunol.* *182*, 2102–2112.
- Robertson, J., Haas, C.T., Pele, L.C., Monie, T.P., Charalambos, C., Parkes, M., Hewitt, R.E., and Powell, J.J. (2016). Intestinal APCs of the endogenous nanomineral pathway fail to express PD-L1 in Crohn's disease. *Sci. Rep.* *6*, 26747.
- Ruane, D.T., and Lavelle, E.C. (2011). The role of CD103+ dendritic cells in the intestinal mucosal immune system. *Front. Immunol.* *2*, 25.
- Salmon, H., Idoyaga, J., Rahman, A., Leboeuf, M., Remark, R., Jordan, S., Casanova-Acebes, M., Khudoynazarova, M., Agudo, J., Tung, N., et al. (2016). Expansion and Activation of CD103(+) Dendritic Cell Progenitors at the Tumor Site Enhances Tumor Responses to Therapeutic PD-L1 and BRAF Inhibition. *Immunity* *44*, 924–938.
- Scanduzzi, L., Ghosh, K., Hofmeyer, K.A., Abadi, Y.M., Lázár-Molnár, E., Lin, E.Y., Liu, Q., Jeon, H., Almo, S.C., Chen, L., et al. (2014). Tissue-expressed B7-H1 critically controls intestinal inflammation. *Cell Rep.* *6*, 625–632.
- Shale, M., Schiering, C., and Powrie, F. (2013). CD4(+) T-cell subsets in intestinal inflammation. *Immunol. Rev.* *252*, 164–182.
- Sharpe, A.H., Wherry, E.J., Ahmed, R., and Freeman, G.J. (2007). The function of programmed cell death 1 and its ligands in regulating autoimmunity and infection. *Nat. Immunol.* *8*, 239–245.
- Shi, Y., and Massagué, J. (2003). Mechanisms of TGF-beta signaling from cell membrane to the nucleus. *Cell* *113*, 685–700.
- Song, M.Y., Hong, C.P., Park, S.J., Kim, J.H., Yang, B.G., Park, Y., Kim, S.W., Kim, K.S., Lee, J.Y., Lee, S.W., et al. (2015). Protective effects of Fc-fused PD-L1 on two different animal models of colitis. *Gut* *64*, 260–271.
- Stolfi, C., De Simone, V., Colantoni, A., Franzè, E., Ribichini, E., Fantini, M.C., Caruso, R., Monteleone, I., Sica, G.S., Sileri, P., et al. (2014). A functional role for Smad7 in sustaining colon cancer cell growth and survival. *Cell Death Dis.* *5*, e1073.
- Tang, Y., Wu, X., Lei, W., Pang, L., Wan, C., Shi, Z., Zhao, L., Nagy, T.R., Peng, X., Hu, J., et al. (2009). TGF-beta1-induced migration of bone mesenchymal stem cells couples bone resorption with formation. *Nat. Med.* *15*, 757–765.
- Tanoue, T., Atarashi, K., and Honda, K. (2016). Development and maintenance of intestinal regulatory T cells. *Nat. Rev. Immunol.* *16*, 295–309.
- Topalian, S.L., Hodi, F.S., Brahmer, J.R., Gettinger, S.N., Smith, D.C., McDermott, D.F., Powderly, J.D., Carvajal, R.D., Sosman, J.A., Atkins, M.B., et al. (2012). Safety, activity, and immune correlates of anti-PD-1 antibody in cancer. *N. Engl. J. Med.* *366*, 2443–2454.
- Tronccone, E., and Monteleone, G. (2019). Smad7 and Colorectal Carcinogenesis: A Double-Edged Sword. *Cancers (Basel)* *11*, E612.
- Wang, P.F., Chen, Y., Song, S.Y., Wang, T.J., Ji, W.J., Li, S.W., Liu, N., and Yan, C.X. (2017). Immune-Related Adverse Events Associated with Anti-PD-1/PD-L1 Treatment for Malignancies: A Meta-Analysis. *Front. Pharmacol.* *8*, 730.
- Wenzel, U.A., Magnusson, M.K., Rydström, A., Jonstrand, C., Hengst, J., Johansson, M.E., Velcich, A., Öhman, L., Strid, H., Sjövall, H., et al. (2014). Spontaneous colitis in Muc2-deficient mice reflects clinical and cellular features of active ulcerative colitis. *PLoS One* *9*, e100217.
- Worthington, J.J., Czajkowska, B.I., Melton, A.C., and Travis, M.A. (2011). Intestinal dendritic cells specialize to activate transforming growth factor- β and induce Foxp3+ regulatory T cells via integrin α v β 8. *Gastroenterology* *141*, 1802–1812.
- Yogeve, N., Frommer, F., Lukas, D., Kautz-Neu, K., Karam, K., Ielo, D., von Stebut, E., Probst, H.C., van den Broek, M., Riethmacher, D., et al. (2012). Dendritic cells ameliorate autoimmunity in the CNS by controlling the homeostasis of PD-1 receptor(+) regulatory T cells. *Immunity* *37*, 264–275.
- Zhang, Y., Chung, Y., Bishop, C., Daugherty, B., Chute, H., Holst, P., Kurahara, C., Lott, F., Sun, N., Welcher, A.A., and Dong, C. (2006). Regulation of T cell activation and tolerance by PDL2. *Proc. Natl. Acad. Sci. USA* *103*, 11695–11700.
- Zou, W., Wolchok, J.D., and Chen, L. (2016). PD-L1 (B7-H1) and PD-1 pathway blockade for cancer therapy: Mechanisms, response biomarkers, and combinations. *Sci. Transl. Med.* *8*, 328rv4.

STAR★METHODS

KEY RESOURCES TABLE

REAGENT OR RESOURCE	SOURCE	IDENTIFIER
Antibodies		
Ultra-LEAF™ purified anti-mouse CD3(17A2)	BioLegend	Cat#100238; RRID: AB_1877072
anti-mouse CD3/FITC(17A2)	BioLegend	Cat#100203; RRID: AB_312660
anti-mouse CD4/APC(GK1.5)	BioLegend	Cat#100412; RRID: AB_312697
anti-mouse CD4/PE (GK1.5)	BioLegend	Cat#116005; RRID: AB_313690
Ultra-LEAF™ purified anti-mouse CD28 (37.51)	BioLegend	Cat#102115; RRID: AB_11150408
anti-mouse PD1/PE(29F.1A12)	BioLegend	Cat#135206; RRID: AB_1877231
anti-mouse PDL1/PE (10F.9G2)	BioLegend	Cat#124308; RRID: AB_2073556
anti-mouse PDL2/PE (TY25)	BioLegend	Cat#107206; RRID: AB_2162011
anti-mouse PDL2/APC	BioLegend	Cat#107210; RRID: AB_2566345
anti-mouse I-Ab/PE (AF6-120)	BioLegend	Cat#116408; RRID: AB_313727
anti-mouse CD103/PE(2E7)	BioLegend	Cat#121406; RRID: AB_1133989
anti-mouse CD103/APC(2E7)	BioLegend	Cat#121414; RRID: AB_1227502
anti-mouse Foxp3/Alexa Fluor 647 (150D)	BioLegend	Cat#320013; RRID: AB_439749
anti-mouse IL-17/APC (TC11-18H10.1)	BioLegend	Cat#506916; RRID: AB_536018
anti-mouse IFN-γ/PE (XMG 1.2)	BioLegend	Cat#505808; RRID: AB_315402
Anti-mouse CD45RB/PE (C363-16A)		Cat#103308; RRID: AB_313015
anti-mouse NK1.1/FITC (PK136)	BioLegend	Cat#108706; RRID: AB_313393
anti-mouse B220/FITC (RA3-6B2)	BioLegend	Cat#103206; RRID: AB_312991
anti-mouse CD11c/APC (N418)	BioLegend	Cat#117310; RRID: AB_313779
anti-mouse CD11c/PE (N418)	BioLegend	Cat#117308; RRID: AB_313777
anti-mouse Phospho-Smad2/3	Cell-signaling Technology	Cat#8828S; RRID: AB_2631089
Experimental Models: Organisms/Strains		
Mouse: B6.Cg-Smad7 ^{tm1.1lnk/J}	Jackson Laboratory	Stock#017008
Mouse: Tg(Cd4-cre)1Cwi/BfluJ	Jackson Laboratory	Stock#017336
Mouse: B6.Cg-Tg(Itgax-cre)1-1Reiz/J	Jackson Laboratory	Stock#008068
Mouse: Pdc1 ^{tm1.1Shr/J}	Jackson Laboratory	Stock#021157
Mouse: B6.129S7-Rag1 ^{tm1Mom/J}	Jackson Laboratory	Stock#002216
Mouse: Foxp3 ^{GFP}	Jackson Laboratory	Stock#006769
Mouse: C57BL/6J	Jackson Laboratory	Stock#000664
Mouse: Smad3 ^{-/-}	Dr. Maggio-Price University of Washington, Seattle	N/A
Experimental Models: Cell Lines		
HEK293	ATCC	ATCC® CRL-1573
Recombinant Proteins		
Mouse PDL1-Fc Chimera Protein, CF	R&D systems	Cat#1019-B7-100
Mouse PDL2-Fc Chimera Protein, CF	R&D systems	Cat#1022-PL-100
GM-CSF	R&D systems	Cat#415-ML-010
IL-4	R&D systems	Cat#404-ML-010
TGF-β	R&D systems	Cat#240-B-002
Chemicals and Peptides		
MOG ₃₅₋₅₅ peptide	Genemed Synthesis Inc	N/A
Dextran Sulfate Sodium Salt (Jaensson et al.)-Colitis Grade (36,000-50,000 MW)	MP Biomedicals	Cat#9011-18-1

(Continued on next page)

Continued

REAGENT OR RESOURCE	SOURCE	IDENTIFIER
Complete Freund's Adjuvant (CFA)	Difco	N/A
Pertussis toxin (PT)	List Biological Laboratories	Cat#180
Critical Commercial Assays		
RNeasy Plus Micro Kit	Qiagen	Cat#74034
RNeasy Mini Kit	Qiagen	Cat#74106
TGF- β BMP Signaling Pathway RT2 Profiler PCR Array	Qiagen	Cat#PAMM-035Z
nCounter [®] Immunology Panel (Mouse)	Nanostring	Cat#XT-CSO-MIMI-12
Naive CD4 ⁺ T cell isolation Kit, mouse	Miltenyi Biotec	Cat#130-104-453
CD11c Microbeads UltraPure, mouse	Miltenyi Biotec	Cat#130-108-338
CD4(L3T4) Microbeads, mouse	Miltenyi Biotec	Cat#130-117-043
Dual-Glo [®] Luciferase Assay System	Promega Corporation	Cat#E2920
Secrete-Pair Gaussia Luciferase Assay Kit	GeneCopoeia	Cat#LF061
eBioscience Foxp3 Transcription Factor staining kit	Thermo Fisher	Cat#00-5523-00
Magna ChIP [™] G- Chromatin Immunoprecipitation kit	EMD Millipore	Cat#17-611
Mouse TGF-beta 1 DuoSet ELISA	R&D systems	Cat#DY1679
Lipofectamine 2000 Transfection Reagent	Thermo Fisher	11668019
Oligonucleotides		
Pdcd1 Forward, GGG AGT CCT TGA GTA TTT GGT GC	Integrated DNA Technologies	N/A
Pdcd1 Reverse, ATG TTT GCT CGG CTT CCT GG	Integrated DNA Technologies	N/A
Pdcdl2 Forward, GGG AGT CCT TGA GTA TTT GGT GC	Integrated DNA Technologies	N/A
Pdcdl2 Reverse, ATG TTT GCT CGG CTT CCT GG	Integrated DNA Technologies	N/A
Itgae Forward, GGG AGT CCT TGA GTA TTT GGT GC	Integrated DNA Technologies	N/A
Itgae Reverse, ATG TTT GCT CGG CTT CCT GG	Integrated DNA Technologies	N/A
Pdcd1 Forward, AGG CCC AGG GTC TTT CTG AA	Integrated DNA Technologies	N/A
Pdcd1 Reverse, TTC AGA AAG ACC CTG GGC CT	Integrated DNA Technologies	N/A
Smad7-antisense 5'-GTC GCC CCT TCT CCC CGC AGC-3'	Integrated DNA Technologies	N/A
Software		
PRISM Version 8	Graphpad	https://www.graphpad.com/scientific-software/prism/
FlowJo Version 10	Tree Star	https://www.flowjo.com/solutions/flowjo/downloads
Adobe Creative Cloud	Adobe	https://www.adobe.com/creativecloud.html
NanoString nSolver 4	NanoString	https://www.nanostring.com/products/analysis-software/nsolver
Aperio eSlide Manager	Leica Biosystems	https://www.leicabiosystems.com/digital-pathology/manage/aperio-eslide-manager/

LEAD CONTACT AND MATERIALS AVAILABILITY

Further information and requests for mouse strains, resources, and reagents should be directed to and will be fulfilled by the Lead Contact, Gopal Murugaiyan, at mgopal@rics.bwh.harvard.edu. This study did not generate other new unique reagents.

EXPERIMENTAL MODEL AND SUBJECT DETAILS

Mice

C57BL/6J WT, Smad7^{fl^{ox}/fl^{ox}}, CD11c^{cre}, CD4^{cre}, Rag-1^{-/-}, and Foxp3^{GFP} mice were purchased from Jackson Laboratory. DC-Smad7^{-/-} (CD11c⁺ dendritic cell Smad7 conditional knockout) mice were created by crossing Smad7^{fl^{ox}/fl^{ox}} x CD11c^{cre} mice. T-Smad7^{-/-} (CD4⁺ T cell Smad7 conditional knockout) mice were created by crossing Smad7^{fl^{ox}/fl^{ox}} x CD4^{cre} mice. Smad3^{-/-} mice were obtained from Dr. Maggio-Price (University of Washington, Seattle). All mice were age- (6–8 weeks old at the start of experiments) and sex-matched (both male and female mice were used). Littermate controls were used where appropriate. Mice were

maintained in specific pathogen-free animal facilities at the Harvard Institutes of Medicine at Harvard Medical School (Boston, MA) and the Hale Building for Transformative Medicine at Brigham and Women's Hospital (Boston, MA). Mice were housed with food and water *ad libitum*. All experiments were in accordance with guidelines from the Institutional Animal Care and Use Committee at Brigham and Women's Hospital.

METHOD DETAILS

DSS-induced colitis

Mice received 3% (36,000–50,000 M.Wt.) DSS (MP Biomedicals) in drinking water for 7 days. Body weight loss as a clinical sign of colitis was recorded daily. Mice that showed excessive body weight loss (> 25%) or signs of rectal prolapse were euthanized. Final body weight scores at euthanasia were recorded for the remainder of monitoring where appropriate. Disease activity index including weight loss, the presence of blood in stool, and stool consistency, was calculated daily as has been previously described (Kim et al., 2012). Each mouse was scored from 0–4 according to the following criteria. **Weight Loss.** 0: < 1%; 1: 1%–5%; 2: 5%–10%; 3: 10%–15%; 4: >15%. **Bleeding.** 0: Normal (hemocult negative, no visible blood in stool); 1: Hemocult positive (hemocult positive, no visible blood in stool); 2: Slightly visible blood in stool (hemocult positive, visible blood in stool with reddish hue upon smear); 3: Visible blood in stool (hemocult positive, obvious blood in stool, but no incrustation around anus); 4: Gross bleeding (fresh extensive blood around anus or encrusted on fur). **Stool Consistency.** 0: Normal (well-formed pellet, solid); 1: Soft (well-formed pellet, soft); 2: Pasty (semi-formed pellet, readily becomes paste upon handling); 3: Loose (poorly formed pellet, readily becomes paste upon handling); 4: Diarrhea (no pellet formation, and/or liquid stools). Guaiac fecal occult blood tests were used to detect blood in stool (ColoScreen, Helena Laboratories). Final scores were determined by summing these three individual scores. Colonic lengths were measured immediately after colons were excised. For histopathological analysis, colons were excised, flushed with PBS, opened longitudinally, arranged in Swiss rolls, and fixed in 10% buffered formalin. They were then embedded in paraffin, sectioned (6–10 μ m), and stained with hematoxylin/eosin (H&E) according to standardized protocols. Sections were blindly scored by a pathologist at the Harvard Rodent Histopathology Core Facility (HRHCF) from 0–4 based on degree of ulceration, loss of crypt architecture, and amount of inflammatory infiltrates. Slides were imaged using an Aperio eSlide Scanner (Leica Biosystems).

Smad7-as and PDL1/2-Fc treatment of colitis

We used a 21-base Smad7 antisense oligonucleotide with the sequence 5'-GTC GCC CCT TCT CCC CGC AGC-3' complementary to the mRNA of Smad7 (purchased from Integrated DNA Technology). The same sequence Smad7-as inhibitor has previously been validated by others *in vitro* and *in vivo* in models of Crohn's disease (CD) (Boirivant et al., 2006) and neuroinflammation (Kleiter et al., 2007), and in CD patients (Monteleone et al., 2001). Mice were treated with Smad7-as or oligonucleotide control inhibitor i.p. (250 μ g/mouse/day) in PBS every other day for four days at the beginning of a 7 day 3% DSS colitis induction, as indicated in Figure 5A. For PDL1/2-Fc treatment, mice were treated with PDL1-Fc, PDL2-Fc, or Ig control (R&D systems) i.p. (20 μ g/mouse/day) every other day for four days at the beginning of a 7 day 3% DSS colitis induction, as indicated in Figure 5A.

CD4⁺CD45RB^{hi} T cell transfer colitis

CD4⁺CD45RB^{hi} T cells were isolated via flow cytometry from donor mice. Recipient Rag1^{-/-} mice were injected i.p. with 5×10^6 T cells and monitored for 7 weeks. Colitis was monitored and scored as detailed above.

EAE

Female mice were injected s.c. into both flanks with 100 μ g MOG_{35–55} peptide (Genemed Synthesis) dissolved in PBS, emulsified in an equal volume of CFA (Difco), supplemented with 5 mg/ml *Mycobacterium tuberculosis* H37Ra. Mice were also injected twice i.p. with 200 ng pertussis toxin (PT) (List Biological Laboratories) administered on the day of immunization and 48 h later. Clinical assessment of EAE was performed daily after disease induction according to the following criteria: 0, no disease; 1, tail paralysis; 2, hind limb weakness or partial paralysis; 3, complete hind limb paralysis; 4, forelimb and hind limb paralysis; 5, moribund state. Mean clinical scores on separate days were calculated by adding the scores of individual mice and dividing by the total number of mice in each group, including mice that did not develop signs of EAE. For histopathological studies, spinal cords were excised, fixed in 10% formalin in PBS, embedded in paraffin, sectioned (6–10 μ m thick), and stained with H&E or Luxol fast blue. Stained sections were evaluated for immune cell infiltration and demyelination by a pathologist at the Harvard Rodent Histopathology Core Facility (HRHCF).

Generation and isolation of DCs and T cells

DCs were derived from bone marrow (BM) progenitor cells. In brief, femoral and tibial cells were harvested in DC culture medium (IMDM medium, 10% FBS, 100 U/ml penicillin, 100 μ g/ml streptomycin, 55 μ M β -mercaptoethanol, 20 ng/mL GM-CSF, and 10 ng/mL IL-4) and seeded in 24-well plates at a density of 1×10^6 cells/ml/well. Culture medium was replaced with fresh medium after 3 days. On days 5–6, dislodged cells were used as BM-derived DCs. Splenic and mesenteric lymph node (MLN) DCs were isolated using magnetic CD11c beads according to the manufacturer's instructions (Miltenyi Biotec) or sorted via flow cytometry. T cells from the lamina propria were isolated from colonic segments as has been previously described (David et al., 2017).

TGF- β ELISA

Ex vivo-isolated DCs were cultured in serum-free media for 60 h. Cell-free supernatants were assayed for TGF- β by ELISA using the mouse TGF- β 1 DuoSet ELISA (R & D systems). For autocrine induction of TGF- β , *ex vivo*-isolated DCs were stimulated with or without TGF- β (0.5 ng/mL) in serum-free media for 12 h, extensively washed, and cultured for another 48 h. Cell-free supernatants were assayed for TGF- β by ELISA.

DC-T cell co-culture

For DC-T cell co-cultures, naive CD4⁺ T cells were isolated from the spleens of Foxp3^{GFP} mice via negative selection of magnetically labeled cells according to the manufacturer's instructions (Naive CD4⁺ T Cell Isolation Kit, Miltenyi Biotec). CD4⁺ T cells were then co-cultured with CD11c⁺ DCs isolated from Smad7^{fl/fl} and DC-Smad7^{-/-} mice at a 1:3 DC:T cell ratio in U-bottom 96-well plates. TGF- β (0.5 ng/mL) was added to Treg-polarizing conditions immediately upon setting DC-T cell co-cultures. All cells were cultured in X-VIVO serum-free media.

T cell culture

For Treg differentiation with T cells alone, plates (96-well flat-bottom) were coated for a minimum of 2 hr at 37°C with anti-CD3 and anti-CD28 (2 μ g/mL), along with either PDL1-Fc or PDL2-Fc (30–100 μ g/mL). Plates were washed with PBS and then T cells were added in the presence or absence of TGF- β (0.5 ng/mL) and cultured for 4 days. All cells were cultured in complete IMDM (IMDM medium, 10% FBS, 100 U/ml penicillin, 100 μ g/mL streptomycin, 55 μ M β -mercaptoethanol). To analyze PD1, plates (96-well flat-bottom) were coated for a minimum of 2 hr at 37°C with low-dose anti-CD3 and anti-CD28 (0.5 μ g/mL). Plates were washed with PBS and then T cells were added in the presence or absence of TGF- β (2.5 ng/mL) and cultured for 18 h.

RNA isolation, cDNA synthesis, and quantitative Real-Time PCR

Total RNA was isolated from cell pellets using the RNeasy Plus Micro Kit (Qiagen) and stored at -80°C . First-strand cDNA synthesis was performed for each RNA sample from 0.5 to 1 μ g of total RNA using Taqman reverse transcription reagents. cDNA was amplified via sequence-specific FAM-labeled primers: IL-17a, Mm00439618_m1; TNF- α , Mm00443258_m1; IL-23, Mm01160011_m1; IL-12, Mm99999066_m1; IL-6, Mm99999064_m1; IL-1 β , Mm01336189_m1; TGF- β , Mm03024053_m1; CD103/Itgae, Mm00434443_m1; IFN- γ , Mm01168134_m1; Foxp3, Mm00475162_m1; IL-18, Mm00434226_m1 (Applied Biosystems) and real-time PCR mix (Applied Biosystems) on an ABI7500 cyclor. GAPDH gene: Gapdh, Mm99999915_g1, was used as an endogenous control to normalize for differences in the amount of total RNA in each sample. All qRT-PCR reactions were performed in duplicate. All values were calculated as fold changes relative to the expression of GAPDH, then presented as fold changes from relevant experimental conditions.

TGF- β signaling in DSS-induced colitis in Smad7^{fl/fl} and DC-Smad7^{-/-} mice was analyzed using the mouse TGF- β BMP Signaling Pathway RT2 Profiler PCR Array (Qiagen). Samples were processed and analyzed according to the manufacturer's instructions.

NanoString

The nCounter Analysis System (NanoString Technologies) utilizes a digital barcode technology for direct multiplexed measurement of analytes and offers high levels of precision and sensitivity, including profiling hundreds of target transcripts from a single sample (<https://www.nanosttring.com>). One hundred ng of RNA per sample were analyzed using the preassembled nCounter Immunology Panels and the nCounter system according to the manufacturer's instructions. Data were normalized and analyzed using nSolver software via the geometric mean of included housekeeping genes. Genes were arranged from most to least upregulated, and a representative selection of relevant genes of interest were shown.

Promoter analysis

In silico promoter analysis: Mouse *Pdcd12*, *Pdcd11*, and *Itgae* promoters were obtained from promoter databases from the UCSC genome browser or CSHL promoter database. These sequences were searched for Smad3 binding sites using PROMO (a web-based algorithm for the prediction of transcription factor binding sites, Alggen: <http://alggen.lsi.upc.es/>) (Farré et al., 2003; Messguer et al., 2002).

ChIP assays

ChIP (chromatin immunoprecipitation) was performed using the Magna ChIP G Kit per the manufacturer's instructions (EMD Millipore, Billerica, MA) with some modifications as described previously (Ajay et al., 2014). Approximately 1×10^6 isolated splenic dendritic cells were treated with 10 ng/mL TGF- β for 12 h. DNA was cross-linked with protein by adding 900 μ L freshly diluted 1% formaldehyde/protease inhibitor in PBS. Sonication was performed to obtain DNA fragments ranging from 200 to 1000 bp. Samples were spun at 10,000xg at 4°C for 10 min, and 500 μ g protein was used in 500 mL volume for IP with 2 μ g SMAD3 or normal rabbit IgG (negative control). Five μ g (1%) of protein from each sample was frozen in 80°C as input. Protein G magnetic bead-antibody/chromatin complex were separated by magnetic rack and washed with 500 mL low-salt immune complex wash buffer, high-salt immune complex wash buffer, LiCl immune complex wash buffer, and tris-ethylenediaminetetraacetic acid buffer. One hundred μ L of ChIP elution buffer/proteinase K was added in IP, as well as input samples, and incubated at 62°C for 2 h with shaking. Proteinase K was denatured by heating at 95°C for 10 min. For IP samples, protein G magnetic beads were separated by a magnetic separator

rack, and supernatant was used for DNA purification. Five μ l of purified DNA was used for real-time PCR using promoter-specific primers of *Pdcd1*, *Pdcdl1*, *Pdcdl2*, *Itgae*, and *Gapdh* (normalizer). Fold calculations were performed and plotted.

Promoter-specific primers used for ChIP assay

Mouse *Pdcdl1*

Forward 5'-GGG AGT CCT TGA GTA TTT GGT GC

Reverse 5'-ATG TTT GCT CGG CTT CCT GG

Mouse *Pdcdl2*

Forward 5'-GGG AGT CCT TGA GTA TTT GGT GC

Reverse 5'-ATG TTT GCT CGG CTT CCT GG

Mouse *Itgae*

Forward 5'-GGG AGT CCT TGA GTA TTT GGT GC

Reverse 5'-ATG TTT GCT CGG CTT CCT GG

Mouse *Pdcd1*

Forward 5' agg ccc agg gtc ttt ctg aa

Reverse 5' ttc aga aag acc ctg ggc ct

Luciferase assays

a. Firefly Luciferase assay: For *Pdcdl1* and *Itgae* luciferase assays, 70%–80% confluent HEK293 cells were co-transfected with pCMV6 or pCMV6 SMAD3, pRL-GAPDH (gift from Dr. Matthias Brock, Center of Experimental Rheumatology, University Hospital Zurich, Zurich, Switzerland) and pGL3*Pdcdl1*Luc or pGL3*Itgae*Luc plasmid using Lipofectamine 2000 transfection reagent (Thermo Fisher Scientific, Waltham, MA per the manufacturer's instruction), washed 6 h post-transfection, and incubated for 48 h. For TGF- β treatment cells were transfected with respective luciferase plasmids and incubated for 24 h. Cells were then treated with 10 ng/mL of TGF- β and incubated for additional 48 h. Then cells were lysed by passive lysis buffer, and luminescence was measured using the Dual-Glo Luciferase Assay System (Promega Corporation) on a Veritas Luminometer (Turner Biosystems, Sunnyvale, CA). *Pdcdl1* and *Itgae* Luciferase readings (Firefly luciferase) were normalized to GAPDH Luciferase (Renilla luciferase) readings, and fold change was calculated compared with control-transfected cells.

b. Secrete pair Gaussia Luciferase (GLuc) assay (Genecopoeia, Rockville, MD)

Measurement of GLuc: For *Pdcdl2* and *Pdcd1* Luciferase activity, we used Secrete Pair Luciferase assay per the manufacturer's instruction. Briefly, HEK293 cells were co-transfected with pCMV6 or pCMV6 SMAD3 and *Pdcd1*GLuc plasmids as described above. TGF- β treatment was performed as described above. After 48 h, 200 μ L of medium was collected. A 100 μ L of Buffer GL-S containing GLuc substrate was incubated for 25 min at room temperature and medium was added to the substrate solution, and luminescence was measured.

Measurement of AP: Fifty μ L of culture medium from GLuc Assay was heated at 65°C for 10 min, and then placed on ice. AP buffer containing AP substrate was added to 10 μ L medium and luminescence was measured. The GLuc measurement was normalized to AP measurements and plotted as fold change to pCMV6- and *Pdcdl2*-transfected control cells. All of these experiments were done in triplicates and luciferase measurements were done in duplicates.

QUANTIFICATION AND STATISTICAL ANALYSIS

Statistics

Statistical analyses were performed using an unpaired 2-tailed Student's t test. A p value of less than 0.05 was considered statistically significant. Data are presented as the mean \pm SEM. For EAE clinical scores and colitis body weight change scores, groups were compared using linear regression analysis. Please see individual figure captions for more details. Nanostring nSolver software was used for Nanostring data analysis. GraphPad Prism 8 software was used for all other analyses.

DATA AND CODE AVAILABILITY

The raw data supporting the current study are available from the Lead Contact upon request. All software is commercially available.

Cell Reports, Volume 28

Supplemental Information

Smad7 Controls Immunoregulatory PDL2/1-PD1

Signaling in Intestinal Inflammation

and Autoimmunity

Lucien P. Garo, Amrendra K. Ajay, Mai Fujiwara, Vanessa Beynon, Chantal Kuhn, Galina Gabriely, Supriya Sadhukan, Radhika Raheja, Stephen Rubino, Howard L. Weiner, and Gopal Murugaiyan

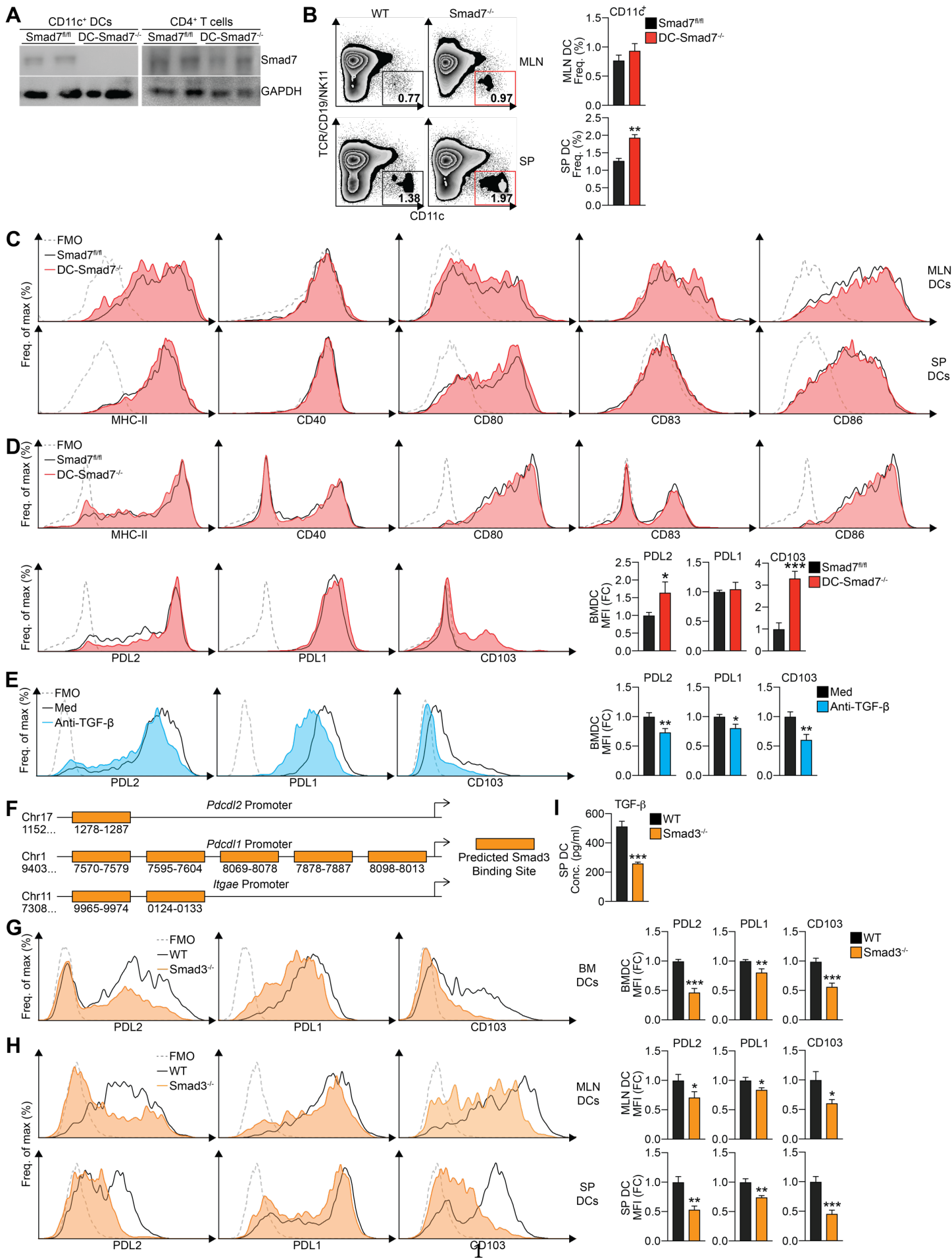


Figure S1. Smad7^{-/-} DCs present with a tolerogenic phenotype, in contrast to Smad3^{-/-} DCs. Related to Figure 1. (A) Western blot of Smad7 in splenic CD11c⁺ DCs (**left**) and CD4⁺ T cells (**right**) isolated *ex vivo* from naïve Smad7^{fl/fl} and DC-Smad7^{-/-} mice. **(B)** Representative FACS plots (**left**) and frequencies (**right**) of CD11c⁺ DCs in the spleens and MLNs isolated *ex vivo* from naïve Smad7^{fl/fl} and DC-Smad7^{-/-} mice (n=6). **(C)** Representative FACS histograms of MHC-II, CD40, CD80, CD83, and CD86 in MLN (**top**) and splenic (**bottom**) DCs from these mice (n=11). **(D)** Representative FACS histograms of MHC-II, CD40, CD80, CD83, CD86, PDL2, PDL1, and CD103 (**top**), and FACS histograms and MFIs of PDL2, PDL1, and CD103 (**bottom**), in BMDCs differentiated from Smad7^{fl/fl} and DC-Smad7^{-/-} mice (n=6). **(E)** Representative FACS histograms (**left**) and MFIs (**right**) of PDL2, PDL1, and CD103 in BMDCs differentiated with or without TGF- β -neutralizing antibody (20 μ g/mL) (n=12). **(F)** Schematic localization of putative Smad3 binding sites on *Pdcd12* (PDL2), *Pdcd11* (PDL1), and *Itgae* promoter regions from Alggen, a web-based algorithm for TFBS predictions. **(G)** Representative FACS histograms (**left**) and MFIs (**right**) of PDL2, PDL1, and CD103 in BMDCs differentiated from WT and Smad3^{-/-} mice (n=11). **(H)** Representative FACS histograms (**left**) and MFIs (**right**) of PDL2, PDL1, and CD103 in MLN (**top**) and splenic (**bottom**) CD11c⁺ DCs from naïve Smad7^{fl/fl} and DC-Smad7^{-/-} mice (n=6). **(I)** ELISA quantification of secreted TGF- β by MLN DCs from these mice (n=4). MFI data reflective of CD11c⁺ population and expressed as fold change (FC) from **(D)** Smad7^{fl/fl} condition, **(E)** media condition, or **(G-H)** WT condition. Data representative of ≥ 3 independent experiments. Mean \pm SEM. *p<.05, **p<.01, ***p<.001, by unpaired T test.

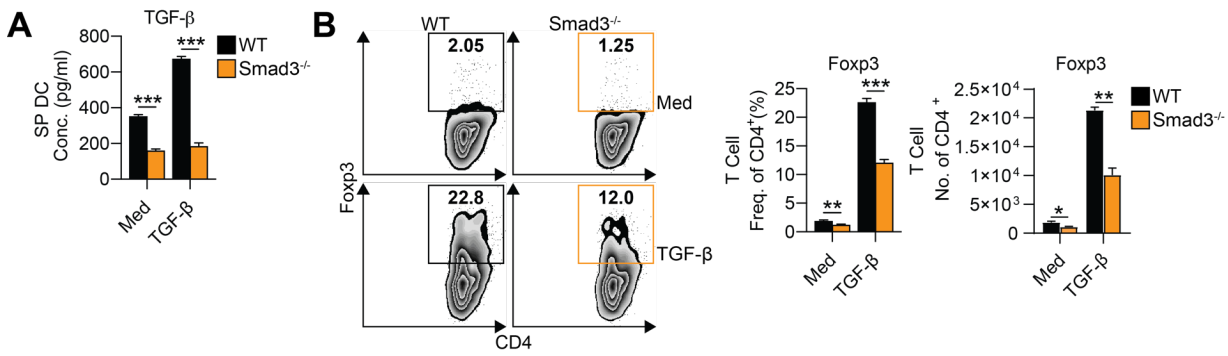


Figure S2. Smad3 promotes DC responsiveness to TGF- β and their ability to induce Tregs. Related to Figure 2. (A) ELISA quantification of secreted TGF- β from splenic WT and Smad3^{-/-} CD11c⁺ DCs stimulated with or without TGF- β (0.5 ng/mL) for 12h, washed and cultured for another 48 h (n=6). **(B)** Representative FACS plots (**left**), frequencies (**middle**), and cell count per well (**right**) of Foxp3-GFP⁺ populations in naïve CD4⁺ Foxp3-GFP T cells co-cultured with splenic CD11c⁺ DCs from Smad7^{fl/fl} or DC-Smad7^{-/-} mice at a 1:3 DC:T cell ratio, with or without TGF- β (0.5 ng/mL), for 4 d (n=4). Data representative of ≥ 3 independent experiments. Mean \pm SEM. *p<.05, **p<.01, ***p<.001, by unpaired T test.

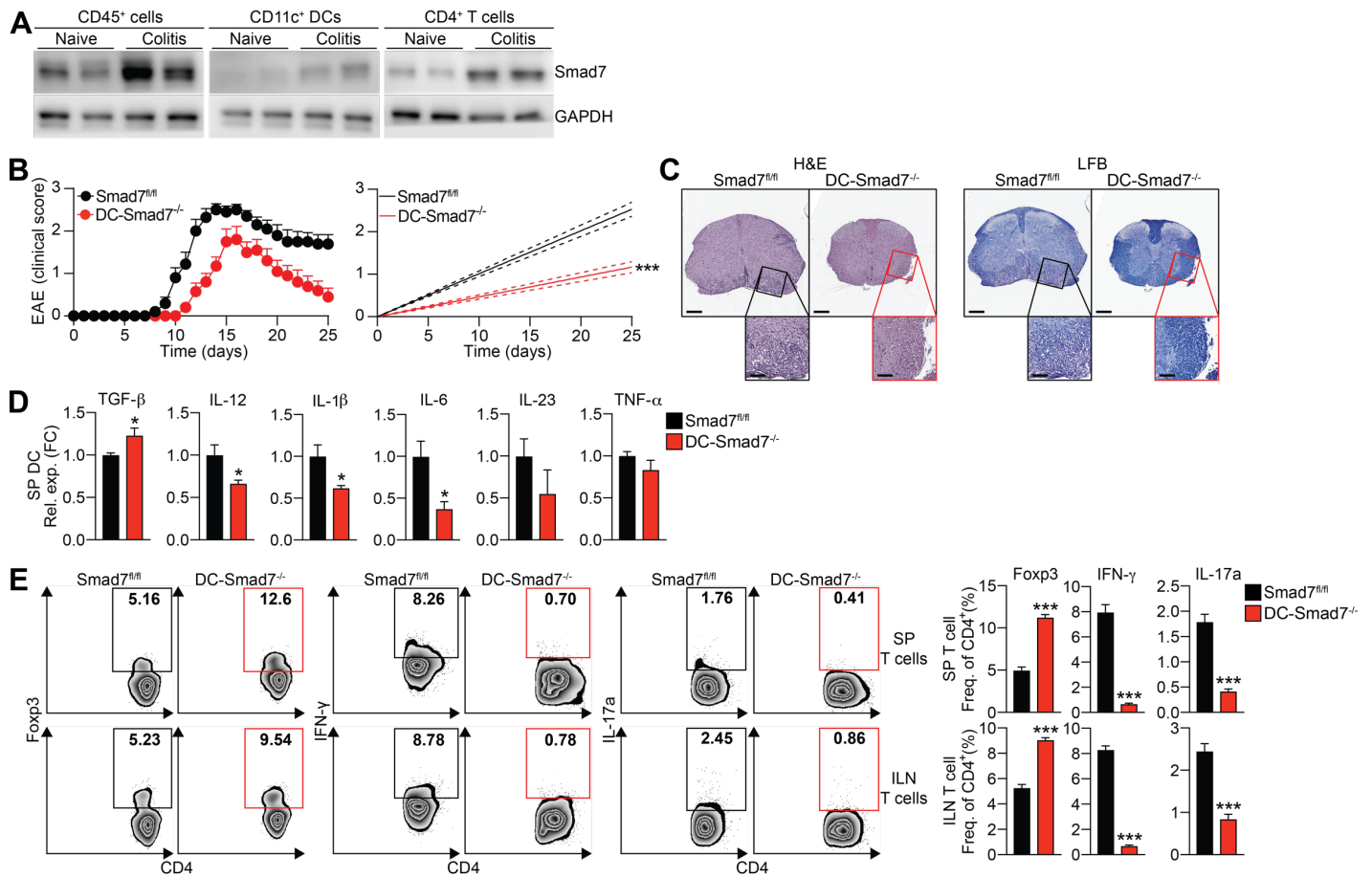


Figure S3. Smad7 is increased during colitis, and Smad7-deficiency in DCs mitigates EAE. Related to Figure 3. (A) Western blot of Smad7 in MLN CD45⁺ cells (left), CD11c⁺ DCs (middle), and CD4⁺ T cells (right) isolated *ex vivo* from naïve and colitic WT mice after 7 days of 3% DSS in drinking water. (B) Clinical EAE scores (left) and linear regression analysis (right) of Smad7^{fl/fl} and DC-Smad7^{-/-} mice immunized with MOG/CFA (n=10). (C) Representative histopathological sections of spinal cords stained with H & E (left) showing inflammatory infiltrates and Luxol Fast Blue (LFB) (right) showing demyelination of these mice at peak disease. Scale bars represent ~250µm (top) and ~100µm (bottom). (D) qRT-PCR of TGF-β, IL-12, IL-1β, IL-6, IL-23, and TNF-α of splenic DCs in these mice at disease onset (n=3-5). Data expressed as fold change from Smad7^{fl/fl} media condition. (E) Representative FACS plots (left) and frequencies (right) of Foxp3⁺, IFN-γ⁺, and IL-17a⁺ populations in splenic (top) and draining inguinal lymph node (bottom) at disease onset (n=10). Data representative of ≥ 3 independent experiments. Mean ± SEM. *p<.05, ***p<.001 by unpaired T test.

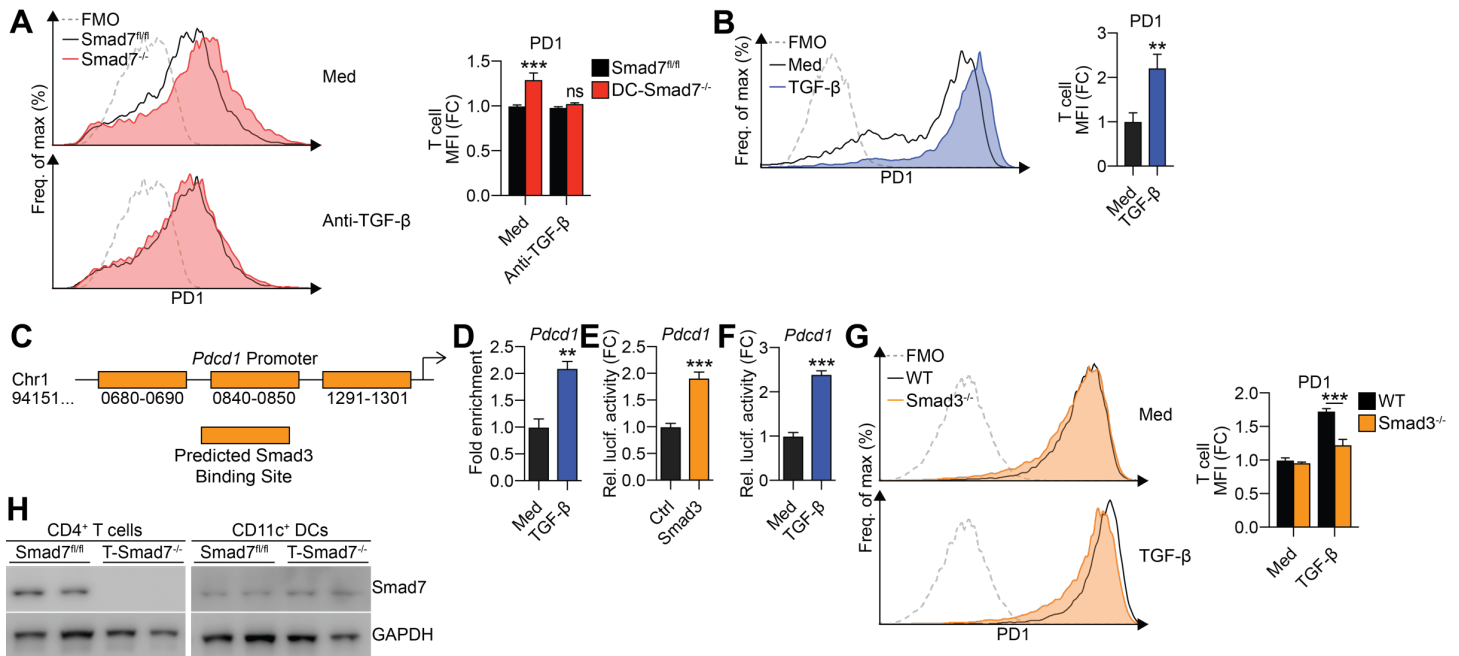


Figure S4. Smad3 promotes CD4⁺ T cell responsiveness to TGF- β and ability to upregulate PD1. Related to Figure 4. (A) Representative FACS histograms (**left**) and frequencies (**right**) of PD1 in naïve CD4⁺ T cells co-cultured with MLN CD11c⁺ DCs from either Smad7^{fl/fl} or DC-Smad7^{-/-} mice with or without anti-TGF- β (10 mg/mL) at a 1:3 DC:T cell ratio, for 18 h (n=6). (B) Representative FACS histograms (**left**) and MFIs (**right**) of PD1 in naïve CD4⁺ T cells stimulated with low-dose anti-CD3 (0.5 μ g/mL) and anti-CD28 (0.5 μ g/mL) with or without TGF- β (2.5 ng/mL) for 18 h (n=10). (C) Schematic localization of putative Smad3 binding sites on *Pdc1* (PD1) promoter region from Alggen, a web-based algorithm for TFBS predictions. (D) ChIP analysis of Smad3 binding promoter region of *Pdc1* in CD4⁺ T cells stimulated with or without TGF- β (10 ng/mL) (n=3). ChIP data expressed as percent fold enrichment as compared to input control. (E) Luciferase reporter activity of *Pdc1* promoter in HEK-293 cells stimulated with control or Smad3 construct or (F) with or without TGF- β (2 ng/mL) (n=6). Luciferase activity represented as relative activity fold change from control or media condition. (G) Representative FACS histograms (**left**) and frequencies (**right**) of PD1 in naïve CD4⁺ T cells from WT and Smad3^{-/-} mice with or without TGF- β (2.5 ng/mL) at a 1:3 DC:T cell ratio, for 18 h (n=6). (H) Western blot of Smad7 in splenic CD4⁺ T cells (**left**) and CD11c⁺ DCs (**right**) isolated *ex vivo* from naïve Smad7^{fl/fl} and T-Smad7^{-/-} mice. Data representative of ≥ 3 independent experiments. MFI data reflective of CD4⁺ population and expressed as FC from (A) Smad7^{fl/fl} media condition, (B) media condition, or (G) WT media condition. Mean \pm SEM. ns, **p<.01, ***p<.001 by unpaired T test.

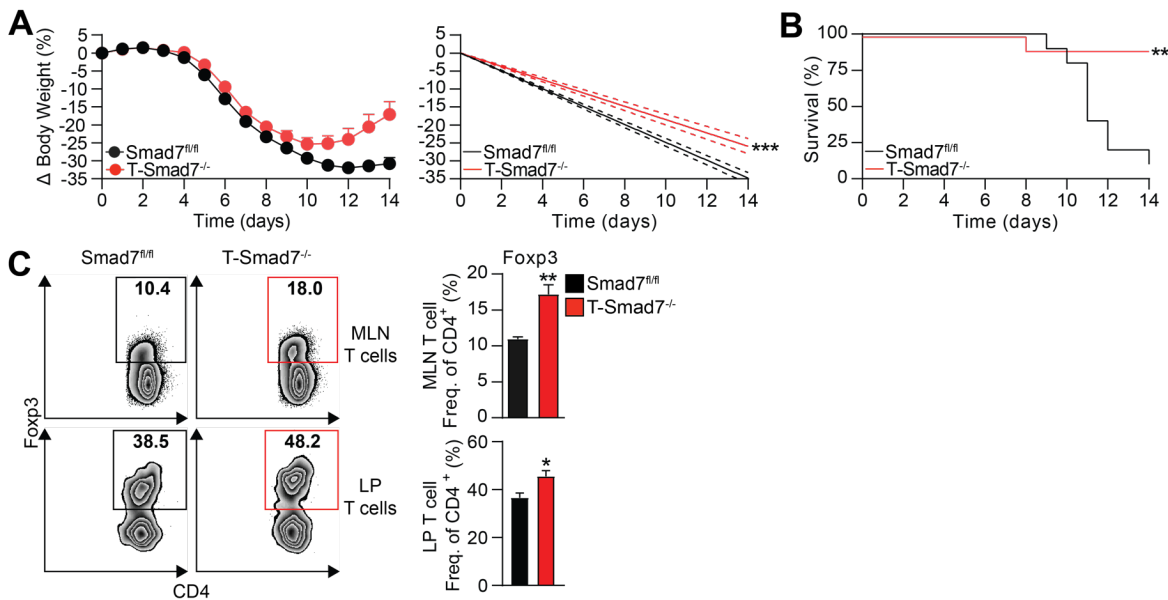


Figure S5. Smad7 deficiency in T cells protects against DSS-induced colitis. Related to Figure 4. (A) Percent body weight changes (left) and linear regression analysis (right) of Smad7^{fl/fl} and T-Smad7^{-/-} mice treated with 3% DSS in drinking water for 7 d, followed by untreated water for 7 d (n=10). The lowest final body weight score for mice that did not survive treatment was recorded for subsequent days until cessation of monitoring. (B) Survival rate of these colitis mice. (C) Representative FACS plots (left) and frequencies (right) of Foxp3⁺ populations in MLN (top) and LP (bottom) CD4⁺ T cells in these mice after 7 days of DSS (n=5). Data representative of ≥ 3 independent experiments. Mean \pm SEM. *p<.05, **p<.01, by unpaired T test.